Anonymous Referee #1

The authors have correctly identified a need to examine long-term ozone records in the Intermountain West to determine if oil and natural gas extraction (O&NG) is having an impact on ozone. However, this paper is overly ambitious and attempts to explore a wide range of potential influences on ozone at 13 rural sites across the Intermountain West. The result is not convincing at all, as the analyses do not have the depth required to understand the observed ozone variability. My recommendation to the editor is that the paper be rejected on the grounds that the conclusions cannot be supported by the thin evidence provided. I encourage the authors to pursue the general theme of the paper but to focus on just one or two sites and conduct a very thorough and indepth analysis of the transport, weather and emissions influences on the interannual variability and trends of ozone. Once the methodology has been developed for one or two sites then the authors could produce a follow-up paper that applies the methods to all 13 sites.

We would like to thank the reviewer for their constructive comments. There appeared to be a fundamental difference of opinion between the reviewer and us regarding the approach to the topic of this work. We took the difference to heart and made substantial revisions of the manuscript to better focus and clarify the key findings, and strengthen the support of the major points. Hopefully through these efforts we were able to better communicate our work now.

Having said that, we respectfully disagree that the analysis in the paper is not thorough and in-depth. It is not clear to us specifically which part of the analysis appeared to be "thin" and "unconvincing" to the reviewer. It is not clear to us what the reviewer meant by "methodology". By virtue of carefully investigating how each of the potential factors may have impacted Intermountain West surface O_3 using a suite of statistical and modeling approaches combined with a synthesis of long-term continuous measurement data, field campaign data, and satellite retrievals, we did develop well-thought out methodology. Such a data analysis approach has been commonly practiced in the literature and in our own decades-long careers. To name a few, Cooper et al. (2012), Parrish et al. (2013) , Mao and Talbot (2004), Mao et al. (2006), Mao et al. (2008), Mao et al. (2017), Zhou et al. (2017), Benedict et al. (2019), Swarthout et al. (2013), Russo et al. (2010a, b), and White et al. (2008), all used similar methodology. The reviewer also suggested using one or two sites for analysis. Our use of all available 11 sites aimed to identify potential patterns of the impact of O&NG emissions, and further, results from 11 sites should be more robust and regionally representative than from only one or two sites.

The goal of this paper is to identify and understand what drives the long-term trends and variability in Intermountain West surface O_3 near O&NG extraction fields. Bearing this goal in mind, we investigated various processes that may have contributed to shaping the long-term variation. In Section 3, we first examined the decadal trends in the annual fourth-highest daily maximum 8-hour average (A4DM8HA) O_3 at 11 sites near O&NG production fields and 2 reference sites. The 2 reference sites were identified by rigorous examination, and they are the only 2 sites located upwind of O&NG extraction fields under minimal influence of anthropogenic emissions from the Intermountain West. No trends in the A4DM8HA O_3 mixing

ratios observed at both sites suggest that the decade of 2005 – 2015 saw relatively constant A4DM8HA O_3 mixing ratios without apparent influence of O&NG emissions over the Intermountain West. Their interannual variability was driven by precipitation weather, wildfire emissions, stratospheric intrusion, and regional transport from the Arctic and the West Coast (Sections 5 – 6 and S5; Lines 484 – 488). What was intriguing was that the 8 sites, with long enough data records for estimates of trends, in the vicinity of O&NG fields have shown largely disparaging long-term trends with some sites showing decreasing trends, some no trends, and others increasing trends, and the trends differed by season. Such a highly heterogeneous spatial pattern of trends strongly suggests that the impacts of O&NG emissions were not straightforward. Therefore, in Sections 4 – 6 together with the Supplement, we investigated factors controlling the significant decreasing trends observed at the Mesa Verde National Park (MEVE), Canyonlands National Park (CANY), and Wind Cave National Park (WICA) and the strong interannual variability in seasonal 5^{th}, 50^{th}, 95^{th} DM8HA O_3 at other sites. Since different processes can be dominant in different seasons, we focused on the contrasting winter and summer seasons for this mechanistic study.

Specifically, in Section 4, we examined *the influence of anthropogenic emissions* by studying annual O&NG production, OMI-retrieved tropospheric NO_2 column densities, and anthropogenic NO_x emissions from National Emission Inventory (NEI) in each O&NG extraction basin. The decreases in natural gas production and coal-fired electricity generation were found to drive the significant decreasing trends at MEVE and CANY, respectively. In Section 5, we studied *the interannual variability of summertime DM8HA* O_3 by examining changes in relative humidity, precipitation rates, and solar radiation at each site. It was found that reduced solar radiation flux with increased cloudiness and precipitation resulted in the significant decreasing trend in the A4DM8HA O_3 at WICA. In Section 6, we identified the close linkage between *wintertime* O_3 *and the Arctic Oscillation (AO),* which had not been studied previously in the decadal context in the literature. At sites located outside the basins, backward trajectory simulations and analysis of potential vorticity suggested that the high O_3 in negative AO years were a result of transport from the Arctic or California and stratospheric intrusion. For sites located within the basins, it was related to strong in situ photochemical production. More importantly, using box model simulations in Section 7, we determined the O_3 *formation regimes* under the influence of the AO. Indeed episodes of high wintertime O_3 in the Intermountain West have been studied using field campaign data. However, to the best of our knowledge, <u>no studies</u> have used those field campaign data in the context of potential influence of O&NG emissions on O_3 formation regimes on decadal scales. The results of this study can provide useful insight for designing a cost-effective O_3 reduction strategy when accounting for the role of AO in the Intermountain West.

We are fully aware that conducting three-dimensional chemistry transport model simulations would be an ideal approach to separate and quantify the effect of each factor (i.e., transport, weather, emissions) on O_3. However, there are undocumented O&NG emission sources and huge uncertainties in existing O&NG emissions, and thus results of model simulations can be difficult to interpret. Therefore, in our opinion, in-depth data analysis using measurement observations has its own advantages in identifying and understanding what drives the long-

term trends and variability in Intermountain West surface O_3 near O&NG extraction fields. As stated in Lines 654 – 656, detailed multiyear studies that integrate measurements and three-dimensional chemical transport model simulations with accurate emission inventories are needed in the future to quantify the contribution of each process identified in this work.

The authors have chosen the annual 4th highest MDA8 ozone value (A4DM8HA) as the metric to explore ozone trends at the rural sites and they then attempt to understand the factors that affect the trends. While A4DM8HA is of interest because it is directly relevant to the NAAQS for ozone, it's not a good metric for understanding processes. This is because the 4th highest value is just one daily measurement per year and it can be influenced by regional scale pollution, long range transport (urban or forest fire plumes) and by stratospheric intrusions. To try to understand the trend in 10 values (one value per year) in the face of such high variability just isn't feasible. I illustrate this limitation by considering the 2005-2015 trend at Mesa Verde National Park (MEVE) in southwestern Colorado. The negative trend in the A4DM8HA at MEVE is largely driven by the very high value in 2005. This trend is a major motivation for the paper but the authors provide no detailed analysis to explore the causes of this trend or to even describe the transport and weather conditions associated with the high ozone events at MEVE. For example, I went to the TOAR database (https://join.fz-juelich.de/access/db/) and very quickly plotted the MDA8 ozone values for every day at MEVE. In 2005 there was a 4-day period in July with ozone over 70 ppbv. It would be very easy to conduct a focused transport analysis of this period to see if ozone precursors were transported from O&NG regions. But the 4th highest value for this year actually occurred on May 16 (76 ppb). What was the cause of this springtime peak? Was it due to O&NG, or was it a stratospheric intrusion? Similarly in 2006 the 4th highest value occurred on May 11. Given that this site experiences high ozone events in spring and summer, with the potential for very different processes controlling these events, the authors should focus their attention on specifically analyzing the situations for each A4DM8HA event in each year. I think they will find that this metric is too erratic for use as an indicator of O&NG emissions from basins that are nearly 100 km away. A better method would be to study the transport, weather and emissions associated with the 20 highest events at MEVE each year (roughly the 95th percentile) to then see if O&NG has a clear association to ozone pollution events at this site. There are 8 additional ozone monitors surrounding Mesa Verde, some in remote areas and others in the oil and gas extraction regions, all available from the TOAR database. Data from these sites can be used to help determine if MEVE is affected by O&NG.

While we greatly appreciate and do agree with some of the reviewer's points, it is also worth noting that the primary metric used by the National Park Service (NPS) is the A4DM8HA, and subsequently the design value, as this is the only regulatory lever that can effectively be used to implement and guide change regarding ozone levels that exceed the National Ambient Air Quality Standards (NAAQS). Therefore, an emphasis has been placed on this metric in this analysis in order to be policy relevant for federal agencies. **Therefore, we devoted Section 3 to addressing anthropogenic influence using this metric in order to be policy relevant for federal agencies. We must note that for analysis of all other factors/processes in the remaining sections, we used seasonal 5th, 50th, and 95th percentile values.**

The US has a long standing commitment to clean, clear air, especially in our national parks. However, many national parks are threatened by elevated levels of air pollution. Air pollutants can adversely impact air quality, diminish visibility, impact ecosystems (such as vegetation, soils, streams, and wildlife), and harm human health. The National Park Service is mandated under the Clean Air Act and the NPS Organic Act to protect air quality and resources that might be adversely affected by air pollution. This is especially true for designated federal Class I areas, of which there are 10 Intermountain West Class I areas used in this study (see Table 1), as these areas have the highest level of air quality protection under the Clean Air Act. For O_3 monitoring, the NPS compares its ambient O_3 concentration data to the primary and secondary NAAQS in order to determine regulatory compliance, as well as for planning and decision making processes used to protect human health and park resources.

From a federal agency standpoint, it is necessary not only to investigate O_3 levels on a percentile basis in order to understand the variability and drivers of elevated O_3 events, as noted by the reviewer, but also to have an in-depth analysis of the A4DM8HA, as this is effectively the only regulatory lever that can be used to implement and guide change. As the principle metric used by park and other land managers, the A4DM8HA is used to examine what is impacting these sites, as well as the region, in order for legally defensible and scientifically sound actions to be carried out with the goal of improving overall air quality. To highlight how integral the A4DM8HA is to assessing air quality in national park units, we have included some links that expand upon the need and use of this metric to the NPS (e.g., Park Conditions and Trends, Natural Resource Condition Assessments, Resource Stewardship Strategies, etc.) and encourage the reviewer to peruse these sites:

- https://www.nps.gov/subjects/air/analysis-methods.htm
- https://www.nps.gov/subjects/air/planningresources.htm
- https://www.nps.gov/subjects/air/park-conditions-trends.htm
- https://www.nps.gov/subjects/air/humanhealth-ozone.htm
- https://www.nps.gov/subjects/air/nature-ozone.htm
- https://sites.google.com/a/nps.gov/resource-stewardship-strategy/anniversary?pli=1
- https://www.nps.gov/orgs/1439/nrca.htm

The initial purpose of this paper was to provide policy-related insight that would be useful for federal agencies like the NPS. As outline above, the A4DM8HA is the metric the Environmental Protection Agency (EPA) uses to implement the NAAQS for O_3. The vulnerable population is most sensitive to this value, and therefore an emphasis on A4DM8HA is highly relevant to policies as well as public interests and welfare. While A4DM8HA ($\sim 99^{th}$ percentile) could be affected by other factors (i.e., stratospheric intrusion and long-range transport), it was more likely to show the effect of local anthropogenic emissions on its decadal trend. Since there are no major local anthropogenic emission sources near O&NG extraction field in the Intermountain West, it is more likely to detect the effect of O&NG emissions, if there was any, on high O_3 levels like A4DM8HA O_3 mixing ratios. For example, *as the reviewer pointed out,*

the decreasing trend in the A4DM8HA at MEVE was likely associated with episodic stratospheric intrusion events in 2005. Mann-Kendall analysis indicated that A4DM8HA O_3 at MEVE over 2006 – 2015 still showed a statistically decreasing trend of -0.52 ppbv/yr ($p = 0.04$). Worth noting, this result is consistent with the NPS Park Conditions & Trends analysis that uses the Kendall-Theil method for this same time period (slope = -0.5 ppbv/yr and is denoted as a significant trend ($p \leq 0.10$)) (https://www.nps.gov/subjects/air/park-conditions-trends.htm). While factors like stratospheric intrusion and long-range transport could cause high A4DM8HA in one/two years, the major cause of its decadal trend has to be associated with local anthropogenic emissions that constantly affected DM8HA O_3. More importantly, we found solid evidence that decreasing emissions from O&NG extraction was the major driving cause for the decadal trend in the A4DM8HA.

It is **NOT** true that we did not provide detailed analysis on the significant decreasing trend in the A4DM8HA at MEVE as well as two other sites (CANY and WICA). We investigated decadal changes in natural gas production, tropospheric NO_2 column densities, and national emissions inventory over each O&NG extraction field to support the effect of O&NG emissions on A4DM8HA O_3 at each site. All sites in this study are rural/remote sites, where O_3 production was generally sensitive to the emission of NO_x (Cooper et al., 2012; Line 276). To study the influence of anthropogenic emissions at the site MEVE, we investigated decadal changes in natural gas production and satellite retrieved tropospheric NO_2 column densities in the San Juan Basin (Lines 272 – 274). A significant decreasing trend of ~ -2.8×10^{13} molecular cm^{-2} yr^{-1} in tropospheric NO_2 column density was observed in the San Juan Basin, which was consistent with decreasing natural gas production in the San Juan County over 2005 – 2015 (Figure 4a). This strongly indicated that decreasing anthropogenic emissions, especially emissions from O&NG extractions, caused the significant the decreasing trend in the A4DM8HA at MEVE.

We agree with the reviewer that decadal trends and interannual variability of A4DM8HA can be influenced by long range transport, stratospheric intrusion, and mostly regional scale pollution. This is ***precisely*** why we examined carefully the role of each process/factor in determining long term trends in seasonal 5^{th}, 50^{th}, and 95^{th} percentile DM8HA O_3 mixing ratios (Sections 5 – 6 and S5). As we pointed out in the Introduction section (Lines 100 – 107), episodic high O_3 events have been studied extensively at sites near O&NG events (e.g., Schnell et al., 2009; Carter and Seinfeld, 2012; Edwards et al., 2014). However, there are only two studies investigating the *long-term* impacts of O&NG extraction activities on surface O_3 and its precursors, which is the vary focus of our study. Individual researchers have their own choices of approach to a scientific problem. We do not disagree with the reviewer's choice of their approach.

The data we used for this study were included in the data the reviewer mentioned in their commentary. Note that the coauthor Dr. B. C. Sive is the Program Manager of the NPS Gaseous Pollutant Monitoring Program; he and his colleagues are who in fact ultimately provided all the NPS data to the TOAR database, which was acquired through the EPA AQS database. Worth noting that the NPS data is most easily accessed through their data request site

(https://ard-request.air-resource.com/). Our selection of the monitoring sties is based on their distances and locations from the O&NG fields in the Intermountain West, which was clearly stated in Section 2.

Other comments:
The opening sentence is almost a verbatim copy of the opening sentence from Cooper et al. [2014]: This work: "Tropospheric ozone (O3) is a short-lived trace gas that either originates naturally from the stratosphere (Stohl et al., 2003) or is produced in situ by photochemical oxidation of nitrogen oxides (NOx) and volatile organic compounds (VOCs) or carbon monoxide (CO) (e.g., Monks et al., 2009)." Cooper et al. [2014]: "Tropospheric ozone is a short-lived trace gas that either originates naturally in the stratosphere (Junge, 1962; Danielsen, 1968; Stohl et al., 2003) or is produced in situ by photochemical reactions involving sunlight and ozone precursor gases including nitrogen oxides (NOx) and non-methane volatile organic compounds, methane (CH4) or carbon monoxide (The Royal Society, 2008; Monks et al., 2009)."
Cooper, O. R., D. D. Parrish, J. Ziemke, N. V. Balashov, M. Cupeiro, I. E. Galbally, S. Gilge, L. Horowitz, N. R. Jensen, J.-F. Lamarque, V. Naik, S. J. Oltmans, J. Schwab, D. T. Shindell, A. M. Thompson, V. Thouret, Y. Wang, R. M. Zbinden (2014), Global distribution and trends of tropospheric ozone: An observation-based review, Elem Sci Anth, 2:29, DOI: http://doi.org/10.12952/journal.elementa.000029

Changed to 'Tropospheric ozone (O_3) is a serious air pollutant that can be harmful to human and ecosystem health. Stratospheric intrusion and in situ photochemical oxidation of nitrogen oxides (NO_x), volatile organic compounds (VOCs), or carbon monoxide (CO) are two sources of tropospheric ozone (e.g., Stohl et al., 2003; Monks et al., 2009).' (Lines 85 – 89).

Line 515 "This study is the first one to investigate the long term impact of O&NG extraction activities on the distribution and trend of surface O3 over the intermountain U.S. "This statement is not entirely true as Bien and Helmig recently explored ozone trends across Colorado to look for an impact from oil and gas emissions. Bien, T. and Helmig, D., 2018. Changes in summertime ozone in Colorado during 2000–2015. Elem Sci Anth, 6(1), p.55. DOI: http://doi.org/10.1525/elementa.300
The text was revised to:

'To the best of our knowledge, only two studies investigated the long-term impact of O&NG extraction on the trend of surface O_3 and its precursors (Majid et al., 2017; Bien and Helmig, 2018). Majid et al. (2017) investigated the decadal trends in OMI-retrieved NO_2 in 7 main shale plays over 2005 – 2015 and found O&NG industry was reversing the rate of changes in NO_2. Bien and Helmig (2018) found surface O_3 at sites within O&NG production basins can be ranked among top ten of all Colorado sites, and further suggested the need of more continuous measurements within O&NG basins to study the long-term influence of O&NG emissions.' (Lines 638 – 645)

Line 66 "Thus, long range transport from Asia and stratospheric intrusion may not be the sole

contributors to the observed increasing trends in western U.S." The latest update on rural ozone trends across the western USA shows that since the year 2000, ozone has begun to decrease in summer [Jaffe et al., 2018]. Jaffe, D. A., et al. (2018), Scientific assessment of background ozone over the U.S.: Implications for air quality management, Elem. Sci. Anth., 6(1):56, DOI:http://doi.org/10.1525/elementa.309

Jaffe et al. (2018) found that A4DM8HA O_3 at most rural and urban sites in the U.S. showed a consistent downward trend since 2000. However, long range transport from Asia and stratospheric intrusion caused the increasing trends in background O_3 in the western U.S. (e.g., Cooper et al., 2012; Parrish et al., 2012; Lin et al., 2017). Since our study was focused on trends in A4DM8HA O_3, discussions on background O_3 were deleted from the manuscript (Lines 76 – 83).

Line 92 Here the authors state that 6 sites in Gaudel et al [2018] show increasing ozone, in winter in the inter-mountain west. But it's not clear which sites they are talking about or how they define the intermountain west. I count more than 6 sites in Gaudel et al. with increasing ozone.

In Figure 14b in Gaudel et al., 2018, daytime average O_3 in winter showed statistically increasing trends at 3 sites near Denver, 1 site to the south of Denver and 1 site near MEVE. To avoid ambiguity, we changed it to:

'Gaudel et al. (2018) assessed surface O_3 trends at 2702 non-urban sites and did not find trends at sites including MEVE, PNDE, YELL in winters of 2000 – 2014.' (Lines 236 – 240).

Line 199 These science questions are in the wrong place and they need to appear at the end of the Introduction as the motivation for this study.

Those questions were raised based on the general characteristics found in Lines 205 – 245. In our opinion, it is appropriate to place those questions at the end of Section 3.

Some other recent paper that explore the impact of O&NG on ozone are: Oltmans, S.J., Cheadle, L.C., Johnson, B.J., Schnell, R.C., Helmig, D., Thompson, A.M., Cullis, P., Hall, E., Jordan, A., Sterling, C., McClure-Begley, A., Sullivan, J.T., McGee, T.J. and Wolfe, D., 2019. Boundary layer ozone in the Northern Colorado Front Range in July–August 2014 during FRAPPE and DISCOVER-AQ from vertical profile measurements. Elem Sci Anth, 7(1), p.6. DOI: http://doi.org/10.1525/elementa.345

Cheadle, L.C., Oltmans, S.J., Petron, G., Schnell, R.C., Mattson, E.J., Herndon, S.C., Thompson, A.M., Blake, D.R. and McClure-Begley, A., 2017. Surface ozone in the Colorado northern Front Range and the influence of oil and gas development during FRAPPE/DISCOVER-AQ in summer 2014. Elem Sci Anth, 5, p.61. DOI: http://doi.org/10.1525/elementa.254

Episodic studies were cited in Line 100.

References:

Benedict, K. B., Y. Zhou, B. C. Sive, A. J. Prenni, K. A. Gebhart, E. V. Fischer, A. Evanoski-Cole, A. P. Sullivan, S. Callahan, B. A. Schichtel, H. Mao, Y. Zhou, and J. L. Collett Jr. (2019), Volatile Organic Compounds and Ozone in Rocky Mountain National Park during FRAPPÉ, Atmos. Chem. Phys., 19, 499–521, https://doi.org/10.5194/acp-19-499-2019.

Carter, W. P. L. and J. H. Seinfeld (2012), Winter ozone formation and VOC incremental reactivities in the Upper Green River Basin of Wyoming. Atmospheric Environment, 50, 255-266, https://doi.org/10.1016/j.atmosenv.2011.12.025.

Cooper, O.R., R.S. Gao, D. Tarasick, T. Leblanc, C. Sweeney (2012), Long-term ozone trends at rural ozone monitoring sites across the United States, 1990-2010. J. Geophys. Res. Atmospheres 117, 1990–2010. https://doi.org/10.1029/ 2012JD018261

Edwards, P.M., Brown, S.S., Roberts, J.M., Ahmadov, R., Banta, R.M., DeGouw, J. A., Dubé, W.P., Field, R. A., Flynn, J.H., Gilman, J.B., Graus, M., Helmig, D., Koss, A., Langford, A.O., Lefer, B.L., Lerner, B.M., Li, R., Li, S.-M., McKeen, S. A., Murphy, S.M., Parrish, D.D., Senff, C.J., Soltis, J., Stutz, J., Sweeney, C., Thompson, C.R., Trainer, M.K., Tsai, C., Veres, P.R., Washenfelder, R. a., Warneke, C., Wild, R.J., Young, C.J., Yuan, B., Zamora, R. (2014), High winter ozone pollution from carbonyl photolysis in an oil and gas basin. Nature, 514(7522), 351-354, https://doi.org/10.1038/nature13767.

Lin, M., Horowitz, L. W., Payton, R., Fiore, A. M., and Tonnesen, G. (2017), US surface ozone trends and extremes from 1980 to 2014: quantifying the roles of rising Asian emissions, domestic controls, wildfires, and climate, Atmos. Chem. Phys., 17, 2943-2970, https://doi.org/10.5194/acp-17-2943-2017.

Mao, H., and R. Talbot (2004), O_3 and CO in New England: Temporal variations and relationships, *J. Geophys. Res., 109*, D21304, doi:10.1029/2004JD004913.

Mao, H., R. Talbot, D. Troop, R. Johnson, S Businger, and A. M. Thompson (2006), Smart balloon observations over the North Atlantic: O_3 data analysis and modeling, *J. Geophys. Res., 111,* D23S56, doi:10.1029/2005JD006507.

Mao, H., R. Talbot, J. M. Sigler, B. C. Sive, and J. D. Hegarty (2008), Seasonal and diurnal variation in Hg° over New England, *Atmos. Chem. Phys., 8*, 1403-1421.

Mao, H., Hall, D., Z. Ye, Y. Zhou, F. Dirk, and L. Zhang (2017), The Impact of Large-Scale Circulation on Regional versus Local Contribution to Ambient Concentrations of Gaseous Elemental Mercury in urban New York, USA, *Atmos. Chem. Phys.*, 17, 11655-11671.

Parrish, D.D., Law, K.S., Staehelin, J., Derwent, R., Cooper, O.R., Tanimoto, H., Volz-Thomas, a., Gilge, S., Scheel, H.E., Steinbacher, M., Chan, E. (2012), Long-term changes in lower tropospheric baseline ozone concentrations at northern mid-latitudes. Atmospheric Chem. Phys. 12, 11485–11504. https://doi.org/10.5194/acp-12-11485-2012

Parrish, D.D., K.S. Law, J. Staehelin, R. Derwent, O.R. Cooper, H. Tanimoto, A. Volz-Thomas, S. Gilge, H.E. Scheel, M. Steinbacher, E. Chan (2013), Lower tropospheric ozone at northern midlatitudes: Changing seasonal cycle. Geophys. Res. Lett. 40, 1631–1636. https://doi.org/10.1002/grl.50303

Russo, R. S., Y. Zhou, M. L. White, H. Mao, R. Talbot and B. C. Sive (2010), Seasonal variation of nonmethane hydrocarbons and halocarbons in New Hampshire: 2004-2006,

Atmos. Chem. Phys., 10, 1-21.
Russo, R. S., Y. Zhou, K. B. Haase, O. W. Wingenter, E. K. Frinak, H. Mao, R. W. Talbot, and B. C. Sive (2010), Temporal variability, sources, and sinks of C1-C5 alkyl nitrates in Coastal New England, Atmos. Chem. Phys., 10, 1865-1883.
Schnell, R. C., Oltmans, S. J., Neely, R. R., Endres, M. S., Molenar, J. V., and White, A. B. (2009), Rapid photochemical production of ozone at high concentrations in a rural site during winter. Nature Geoscience, 2, 120-122, https://doi.org/10.1038/ ngeo415.
Swarthout, R. F., Russo, R. S., Zhou, Y., Hart, A. H., and Sive, B. C. (2013), Volatile organic compound distributions during the NACHTT campaign at the Boulder Atmospheric Observatory: Influence of urban and natural gas sources, J. Geophys. Res.-Atmos., 118, 10614–10637, https://doi.org/10.1002/jgrd.50722.
White, M., R. S. Russo, Y. Zhou, R. K. Varner, L. C. Nielsen, J. Ambrose, O. W. Wingenter, K. Haase, R. Talbot and B. C. Sive (2008), Volatile organic compounds in northern New England marine and continental environments during the ICARTT 2004 campaign, J. Geophys. Res., 113, D08S90, doi:10.1029/2007JD009161.
Zhou, Y., H. Mao, K. Demerjian, C. Hogrefe, and J. Liu (2017), Regional and Hemispheric Influences on Temporal Variability in Baseline Carbon Monoxide and Ozone over the Northeast US, *Atmos. Environ.*, 164, 309-324.

Decadal Trends and Variability in Intermountain West Surface Ozone near Oil and Gas Extraction Fields

Ying Zhou[1], Huiting Mao[1], and Barkley C. Sive[2]

[1]Department of Chemistry, State University of New York College of Environmental Science and Forestry, Syracuse, NY, 13210, USA

[2]National Park Service, Air Resources Division, Lakewood, CO 80225, USA

Corresponding author: H. Mao (hmao@esf.edu)

Abstract

Decadal trends in ~~the annual fourth-highest daily maximum 8-hour average (A4DM8HA)~~surface ozone (O_3) were studied ~~over 2005 – 2015~~ for ~~13 rural/remote sites in~~ the U.S. Intermountain West~~.~~ ~~No~~ over 2005 – 2015. Widely disparaging trends, or a lack thereof, were ~~observed in A4DM8HA O_3~~found at ~~two reference~~8 sites, ~~which are located upwind of and thus minimally influenced by emissions from~~with sufficiently long data records, in/near oil and natural gas (O&NG) basins~~.~~ ~~Trends, or a lack thereof, varied widely at other 11 sites in/near O&NG basins~~ resulting from different controlling factors rather than a simplistic, uniform one. ~~The~~Three sites exhibited statistically significant decreasing trends with rates of 0.83 ppbv/yr, -0.58 ppbv/yr, and -1.16 ppbv/yr at Mesa Verde ~~(-0.76 ppbv/yr) and~~ National Park, Canyonlands National Park ~~(-0.54 ppbv/yr)~~, and Wind Cave National Park, respectively. It was found that the decreasing trends at the first two sites were ~~attributed to a 37% decrease in~~driven by decreased natural gas production ~~in the San Juan Basin and 35% emission reductions in~~ and decreased emissions from coal-fired electricity generation~~, respectively. The decreasing~~ nearby, and the trend ~~(-1.21 ppbv/yr)~~ at Wind Cave National Park resulted from reduced solar radiation due to increasingly frequent precipitation weather. The lack of trends at the remaining sites was likely caused by the increasing O&NG emissions and decreasing emissions from other anthropogenic activities. Wintertime ~~O_3~~atmospheric stagnant ~~events~~conditions, often with occurrence of high O_3, were associated with the Arctic Oscillation (AO~~). Box model simulations suggested that both~~) during the decade. Furthermore, emission reductions of volatile organic compounds (VOCs) and ~~nitrogen oxides emission reductions~~ NO_x during negative AO years ~~while~~and VOC emission reductions alone in positive AO years could effectively mitigate high wintertime O_3 within the O&NG basins~~.~~, as indicated by box model simulations. Our findings suggest that emissions from O&NG extraction

~~likely played a significant role in shaping long-term~~activities could alter decadal trends in ~~surface~~Intermountain West O_3 ~~near/within O&NG basins~~design values and hence warrant consideration in ~~the design of~~developing efficient O_3 mitigation strategies for the Intermountain West.

1 Introduction

~~Tropospheric ozone (O_3) is a short-lived trace gas that either originates naturally from the stratosphere (Stohl et al., 2003) or is produced in situ by photochemical oxidation of nitrogen oxides (NO_x) and volatile organic compounds (VOCs) or carbon monoxide (CO) (e.g., Monks et al., 2009). On 1 October 2015, the U.S. Environmental Protection Agency (EPA) lowered the National Ambient Air Quality Standard (NAAQS), namely the O_3 design value, to 70 ppbv to improve protection of public health and welfare (EPA, 2015). Unlike in the eastern U.S., where NO_x emission reductions have led to O_3 declines, in the Intermountain West no decreasing trends were observed over 1988 – 2014 and surface O_3 could exceed the NAAQS in both winter and summer (Schnell et al., 2009; Cooper et al., 2012; Edwards et al., 2014; Lin et al., 2017). Most studies attributed the increasing background O_3 trends over the western U.S. to increasing anthropogenic Asian emissions (e.g., Cooper et al., 2012; Parrish et al., 2012; Lin et al., 2017). Lefohn et al. (2012) found that stratospheric intrusion affected the interannual variability of surface O_3 at both high- and low-elevation sites. However, a multi-model study suggested that surface O_3 in the U.S. was far more sensitive to domestic emission changes than to global emission changes in spring and summer (Reidmiller et al., 2009). Thus, long range transport from Asia and stratospheric intrusion may not be the sole contributors to the observed increasing trends in western U.S.~~

~~Recent expanded use of horizontal drilling and hydraulic fracturing technologies enabled access to more natural gas resources in shale deposits (EIA, 2015).~~ Tropospheric ozone (O_3) is a serious air pollutant that can be harmful to human and ecosystem health. Stratospheric intrusion and in situ photochemical oxidation of nitrogen oxides (NO_x), volatile organic compounds (VOCs), or carbon monoxide (CO) are two sources of tropospheric ozone (e.g., Stohl et al., 2003; Monks

et al., 2009). On 1 October 2015, the U.S. Environmental Protection Agency (EPA) lowered the National Ambient Air Quality Standard (NAAQS), namely the O_3 design value, to 70 ppbv to improve protection of public health and welfare (EPA, 2015). Unlike in the eastern U.S., where NO_x emission reductions have led to declines in higher O_3 mixing ratios, in the Intermountain West no decreasing trends were observed over 1988 – 2014, and surface O_3 exceeded the NAAQS in both winter and summer (Schnell et al., 2009; Cooper et al., 2012; Edwards et al., 2014; Lin et al., 2017).

Recent expanded use of horizontal drilling and hydraulic fracturing technologies enabled access to more natural gas resources in shale deposits (EIA, 2015). Extraction of oil and natural gas (O&NG) can result in the emission of O_3 precursor gases and subsequently episodes of elevated O_3 mixing ratios in O&NG production basins frequently exceeding the NAAQS. (e.g., Schnell et al., 2009; Cheadle et al., 2017; Oltmans et al., 2019). Most notable were the episodes that occurred during the cold season in the Intermountain West (Carter and Seinfeld, 2012; Edwards et al., 2014; Rappenglück et al., 2014; Schnell et al., 2009). Carter and Seinfeld (2012) studied found one of the four observed winter O_3 episodes studied to be highly NO_x-sensitive and the other three VOCs-sensitive in the Upper Green River Basin in Wyoming and found one episode highly NO_x-sensitive and the others VOCs-sensitive.. Edwards et al. (2014) used), using a box model to simulate a stagnant 6-day high winter O_3 event in the Uintah Basin and found, suggested that carbonyl photolysis waswas be the dominant oxidant source. McDuffie et al. (2017) studied O_3 in the Colorado Northern Front Range (NFR) in summer 2012 and foundestimated that O&NG emissions contributed to 17% of the modeled maximum photochemically produced O_3. in the Colorado Northern Front Range in summer 2012. To the best of our knowledge, novery few studies

have investigated the long-term impact of expanded O&NG extraction activities on surface O_3 over the intermountain U.S. using more than ten years of measurement data.

The effect of emissions from O&NG production on surface O_3 is difficult to quantify because a wide range of factors work together to determine the mixing ratio of O_3 at a given location, such as other anthropogenic emissions, natural emissions, transport processes, stratospheric intrusion, O_3 photochemistry, and changing global climate (Parrish et al., 2013~~); however~~). However, the significance of these factors varies by season. For example, the number of high O_3 days in summer was strongly correlated with wildfire burned area over the western U.S. as wildfires are important sources of NO_x, CO, and VOCs (Jaffe et al., 2008; Jaffe and Wigder, 2012). The frequency and intensity of wildfires in the western U.S. may ~~be~~have been increasing, driven by increasing temperatures, earlier snowmelt, drier conditions, and accumulation of fuels (Westerling et al., 2006; Jaffe et al., 2008). Moreover, all components that can impact the distribution of O_3 are associated with varying atmospheric circulation patterns on interannual to decadal ~~time~~ scales (e.g., Lin et al., 2014; Zhou et al., 2017). For instance, model simulations suggested that more frequent stratospheric intrusion events occurred in late spring, when the polar jet meandered towards the western U.S. following La Nina events (Lin et al., 2014). Therefore, it is fundamentally important, yet ~~also~~ challenging, to ~~extract~~delineate the impact of increasing emissions from O&NG production on surface O_3 ~~levels~~ from ~~all of these~~ various factors~~. However, these~~, and the resultant findings could ultimately ~~lead~~contribute to improved modeling and to better assess the efficacy of emission controls.

A most common approach to assess the influence of a certain factor or source on O_3 concentrations is through model simulations (e.g., Rodriguez et al., 2009; Lin et al., 2017). However, the application of current chemical transport models used to investigate the impact of

emissions from O&NG extraction on tropospheric O_3 is particularly challenging because of ~~the large~~incomplete inventories of O&NG emission sources and huge uncertainties in existing ~~in the~~ emission inventories ~~of O&NG extraction~~ (Pétron et al., 2014; Helmig et al., 2014; Ahmadov et al., 2014; Thompson et al., 2017; Allen, 2014; Allen, 2016). ~~Past studies have found that~~A case in point is the largely underestimated emissions of methane and VOCs from ~~oil and gas~~O&NG extraction ~~was largely underestimated (~~as suggested by Karion et al~~.,~~ . (2013~~;~~) and Ahmadov et al~~.,~~ . (2014).~~—~~ Consequently model simulations can be difficult to interpret. Therefore, for this study the approach of *data analysis* was chosen ~~in order~~ to provide measurement-based ~~contribution estimates~~understanding of how O&NG emissions together with various factors may have worked together to shape the long-term variation in Intermountain West surface O_3.

Specifically, we investigated the decadal impact of emissions from O&NG extraction on variability and long term trends ~~of surface O_3~~ in ~~the~~ Intermountain West surface O_3 since 2005, when O&NG extraction activities started to expand rapidly (EIA, 2015). In this study, we used long term O_3 measurement data obtained from the National Park Service ~~(NPS),~~ Clean Air Status and Trends Network ~~(CASTNET),~~ and Wyoming Department of Environmental Quality ~~(WDEQ),~~ many of which are from Class I areas as designated by the Clear Air Act. ~~However, some~~Some of these sites have been reportedly influenced by O&NG emissions since 2005 (EIA, 2015). This study was focused on the summer and winter, when NAAQS exceedances ~~of NAAQS~~ tended to occur in the Intermountain West (Edwards et al., 2014; Lin et al., 2017).

2 Materials and Methods

2.1 Site Selection and Data description

Long term surface O_3 observations were available at 18 sites in remote and rural areas of the U.S. Intermountain West (Figure 1 and Table ~~S1~~1). Among the 18 sites, 11 sites are located within

100 km of a shale play and are more likely affected by emissions from O&NG extraction activities (Figure 1). Specifically, Six sites, Mesa Verde National Park (MEVE), Pinedale, WY (PNDE), Centennial, WY (CNTL), Gothic, CO (GTHC), Rocky Mountain National Park (ROMO), and Wind Cave National Park (WICA)), are located near O&NG Basins*outside* O&NG basins. MEVE was located to the northwest of San Juan Basin, while PNDE was located to the north of Green River Basin. Five sites are located *within* O&NG extraction basins. These five sites are: Canyonlands National Park (CANY),) and Campbell, WY (CAMP), located within the Paradox Basin and Powder River Basin, respectively, Dinosaur National Monument (DINO), Rangely, CO (RANG), Meeker, CO (MEEK), and Campbell, WY (CAMP) are located) within O&NG basins.the Uintah Basin (Figure 1). Of the remaining 7 sites, Yellowstone National Park (YELL) and Craters of the Moon National Monument and Preserve (CRMO) were the only two sites located upwind of O&NG fields and were therefore used as reference sites to investigate the decadal O_3 change with minimal influence of O&NG emissions. Four sites, Great Basin National Park (GRBA),, Zion National Park (ZION),, Grand Canyon National Park (GRCA),, and Petrified Forest National Park (PEFO),, were found, based on backward trajectory cluster analysis, to often receive air masses influenced by nearby anthropogenic emissions from Las Vegas (Section S2). Badlands National Park (BADL),, located more than 100 km away from the shale play, was impacted one third of the time by air masses from O&NG activity in the Powder River Basin during the 2005 – 2015 decade (Section S2). Therefore, GRBA, ZION, GRCA, PEFO and BADLthe above five sites were not included in the analysis of this study.

Continuous hourly measurements of O_3 were available at each site. We calculated the annual fourth-highest daily maximum 8-hour average (A4DM8HA), upon which the O_3 design value was based, for the 13 monitoring sites and their trends were examined through ordinary

~~linear least-square regression.~~. Trends (ppbv yr^{-1}) in A4DM8HA were then reported using Sen's slopes from non-parametric Mann-Kendall analysis. The trends were also calculated separately for 5^{th}, 50^{th}, 95^{th} percentiles of daily maximum 8-hour average (DM8HA) O_3 in winter and summer.

2.2 Box Model Simulations

Box model simulations were performed using BOXMOX (Knote et al., 2015) and the NCAR Tropospheric Ultraviolet and Visible Radiation Model (TUVv5.3.1) (Madronich et al., 1998). BOXMOX is an extension to the Kinetic PreProcessor which allows ~~an~~ easy set~~-~~up for ~~zero dimension~~ box model simulations (Knote et al., 2015). We selected the Master Chemical Mechanism (MCM v3.3) for the model chemistry scheme. The MCM is a near-explicit chemical mechanism including gas-phase tropospheric degradations of 74 VOCs and OVOCs with a total of 5259 species of and 15176 reactions (Jenkin et al., 2015).

All simulations were initialized with observations from field campaigns in the Intermountain West~~.~~ during the study period. These campaigns were Uintah Basin Winter Ozone Study (UBWOS) over 2012 – 2014 (Edwards et al., 2013), Nitrogen, Aerosol Composition, and Halogens on a Tall Tower (NACHTT) in 2011 (Swarthout et al., 2013), and Front Range Air Pollution and Photochemistry Éxperiment (FRAPPÉ) in 2014 (Pfister et al., 2017). Section S8 provides detailed information ~~about~~on field campaign measurements. The modeled mixing ratios of CO, CH_4, NO, NO_2, and non-methane VOCs were forced to match the measured diurnal profiles by introducing turbulent mixing to the model (Knote et al., 2015; Section S8.3). Therefore, the "box" can dynamically exchange with its surroundings. The model was integrated forward with a time step of 10 minutes until the concentrations reach a diurnal steady state, when the cycles of simulated species exhibit less than 0.01% variation from the previous day (Edwards et al., 2013). The last 24

h were used to represent the simulated diel cycles. Section S8 provides further information on the model treatment of all chemical observations.

3. General Characteristics in Long-term Variations of O_3

First, changes in the A4DM8HA ~~were examined for the 13 sites~~from before ~~and~~to after 2005, when O&NG extraction started expanding rapidly, were examined for the 13 sites. Note that trends were not calculated for three sites, DINO, RANG, and MEEK, due to short data records (<6 yrs) or too many missing data. Before 2005, statistically significant increasing trends were observed at the reference site CRMO as well as ~~three other sites,~~ CANY, CNTL, and PNDE, three sites near O&NG basins ~~with~~, and no significant trends were observed at the ~~other~~remaining five sites (Figure 2; Table S1). After 2005, no significant trends were found at the two reference sites (CRMO and YELL, Table ~~S2). Among~~ S1), and decreasing or no trends were found at the ~~11~~eight sites near/within the O&NG basins. Specifically, significant decreasing trends were observed at CANY (-0.~~54~~58 ppbv yr^{-1}), MEVE (-0.~~76~~83 ppbv yr^{-1}), and WICA (-1.~~21~~16 ppbv yr^{-1}), ~~with~~while no significant trends at the other five sites (Table ~~S2~~S1). The decadal mean A4DM8HA O_3 was ~58 ppbv at the urban station CAMP in Colorado (https://www.colorado.gov/airquality) and ~77 ppbv at the urban station Hawthorne in Utah (https://deq.utah.gov/division-air-quality). In comparison, the decadal (2005 – 2015) mean of the A4DM8HA reached or exceeded 70 ppbv, the current NAAQS, at three sites, DINO (82.7 ppbv), RANG (72.7 ppbv), and ROMO (75.1 ppbv).

Trends in seasonal 5^{th}, 50^{th}, 95^{th} percentiles of DM8HA O_3 were further examined for winter and summer seasons (Table ~~S3~~S2). At the two reference sites, no trend was observed in any seasonal percentiles of DM8HA O_3 at YELL, while statistically significant decreasing trends (-0.~~14~~16 to -1.~~18~~30 ppbv yr^{-1}) were observed in wintertime 50^{th}/95^{th} and summertime 5^{th}/50^{th}/95^{th} percentile values at CRMO. Significant decreasing trends were also observed at 4 sites located

in/near O&NG basins. Specifically, at MEVE significant decreasing trends of -0.~~49~~47 to -0.~~63~~69 ppbv yr^{-1} were found in seasonal 50^{th}/95^{th} percentile values in both winter and summer (Table S3). In contrast, significant decreasing trends were only found in summertime 5^{th}/50^{th} at CANY, summertime 95^{th} at WICA, and wintertime 50^{th}/95^{th} percentile values at GTHC. Overall ~~seasonal~~wintertime median values near the O&NG extraction basins showed relatively more consistent patterns of interannual variation with low O_3 values in 2012 and higher O_3 in 2011 and 2013 at relatively low elevation sites (i.e., CANY, DINO, MEEK, RANG, CAMP, MEVE, and WICA) ~~in winter, while in~~(Figure 3). In summer, large differences were found between sites (Figure 3).

Previous studies have examined long term trends in tropospheric O_3 for varying time periods over the continental U.S. (e.g., Cooper et al., 2012; Cooper et al., 2014; Lin et al., 2017; Gaudel et al., 2018). Gaudel et al. (2018) assessed surface O_3 trends at 2702 non-urban sites ~~from the Tropospheric Ozone Assessment Report (TOAR) database. They found significant increasing~~and did not find trends ~~(0.5 to 1.0 ppbv yr^{-1}) in daytime average O_3 at 6 sites in the Intermountain West and no trends at 8 other~~at sites including MEVE, PNDE, YELL in winters of 2000 – 2014 ~~(Gaudel et al. 2018).~~. However, in ~~this~~our study a significant decreasing trend (-0.~~49~~67 ppbv yr^{-1}) in wintertime 95^{th} percentile values was observed at MEVE after 2005, possible causes for which ~~are discussed further~~were examined in Section 4. In summers of 2000 – 2014, significant decreasing trends (~ -0.5 ppbv yr^{-1}) in daytime average O_3 were observed by Gaudel et al. (2018) at most sites including CRMO, PNDE, CANY, MEVE, which was consistent with the trends ~~we~~ observed for our study period 2005 – 2015 (Table S3).

The following questions arose from examining the above characteristics in surface O_3 at the 11 sites near/in O&NG basins:

1) ~~Were~~How were the decreasing trends in A4DM8HA at MEVE, CANY, and WICA ~~potentially~~and no trends at other sites linked ~~in some ways~~ to ~~changes in~~nearby O&NG production activities ~~nearby~~?
2) Was ~~there seasonal variation in~~ the influence of emissions from O&NG extraction on ~~seasonal~~ DM8HA O_3 seasonally variable?
3) Were there changes of O_3 production regime as a result of emissions from O&NG basins over the years?

These questions ~~are~~were addressed in the following sections with the goal to delineate the role of emissions from O&NG production in long-term trends in surface O_3 at the 11 sites.

4. Contribution of emissions from O&NG production vs other anthropogenic sources

The two reference sites, YELL and CRMO, are located >100 km upwind of O&NG basins (Figure 1) and exhibited no trends in A4DM8HA after 2005. In comparison, ~~decadal~~ trends ~~of~~ ~~O_3~~varied widely at the ~~11~~eight sites situated in or near ~~the~~ O&NG extraction basins ~~ranged widely, indicating~~. The following analysis suggests that such varying trends resulted from the complex influence of ~~varying~~ranges of changes in emissions from O&NG production activities combined with other anthropogenic sources.

The four *low*-elevation sites, MEVE, CANY, WICA, and CAMP, were situated near/within O&NG basins, with the first three showing significant decreasing trends and the last none. The strong decreasing trends in A4DM8HA at MEVE and CANY appeared to be driven by significant reductions of emissions from local industry during 2005 – 2015. MEVE is located near the San Juan Basin (Figure 1), the second largest natural gas field in the U.S~~. A~~., where a 37% decrease ~~in~~was reported for its natural gas production ~~was reported in the San Juan Basin~~ over 2005 – 2015 (Figure 4a~~),~~) subsequently leading to reduced emissions of O_3 precursors. Meanwhile NO_x

emissions from other sectors in San Juan County decreased by 65% from 80,734 tons in 2005 to 27,996 tons in 2014 (Table S4). This is supported by the strong declines in tropospheric NO_2 column densities in summer at a rate of ~ -2.8 × 10^{13} molecular cm^{-2} yr^{-1} ($p \leq 0.05$) surrounding MEVE around the San Juan Basin over 2005 – 2015 (Figure 4b). Decadal changes were not computed for winter due to scarce wintertime column NO_2 retrievals over the Intermountain West. Because O_3 production in U.S. rural areas was typically sensitive to changes in NO_x emissions (Cooper et al., 2012), the decreasing NO_x emissions associated with reduced natural gas production and emission controls in other sectors were most likely the primary cause for the significant decrease in the A4DM8HA at MEVE (-0.~~76~~83 ppbv yr^{-1}) during 2005 – 2015. The significant decreasing trend in the A4DM8HA observed at CANY was possibly a result of the declining extraction of coalbed methane (CBM) in the Paradox Basin and emission reductions in coal-fired electricity generation in Emery County. Historically, Emery County in the Paradox Basin was the main CBM producer. ~~Permitting activities for~~ CBM extraction ~~have~~has declined by 48% over 2005 – 2015 resulting from lower natural gas prices (NGI, 2018) (Figure 4a). Meanwhile, NO_x emissions from coal-fired electricity generation, contributing ~88% of the total NO_x emissions in Emery County, decreased by 35% from 28,407 tons in 2005 to 18,336 tons in 2014 (Table ~~S4). As a result of these changes, significant decreasing trends in the seasonal 95th percentile would be anticipated, but were not observed in both winter and summer. This indicates that there are additional factors producing significant influences on O_3 in the area, which are further investigated in Sections 5 – 6.~~S3).

~~No trend was observed in the A4DM8HA O_3 at CAMP, which was~~WICA, located downwind of the Powder River Basin, also experienced a significant decreasing trend in the A4DM8HA at a rate of 1.16 ppbv yr^{-1} (p = 0.09) over 2005 – 2014. Curiously, total NO_x emission

increased by 29% from 1,327 tons in 2005 to 1,712 tons in 2014 in Custer County, where WICA is located (Table S3). The decreasing A4DM8HA at WICA indicates additional factor(s) with significant influences, which were further investigated in Sections 5. CAMP, located within the Powder River Basin, saw no trend in the A4DM8HA O_3, likely associated with changes in natural gas vs. oil production activities in the Powder River Basin. ~~CAMP is located within the~~The Powder River Basin~~, which~~ is traditionally known for its coal production and has been one of the fastest growing oil producing regions in recent years. While natural gas production in Campbell County decreased by 62% (Figure 4a), oil production in Campbell County increased from 9×10^8 barrels in 2005 to 2.3×10^9 barrels in 2015 (http://wogcc.wyo.gov/). ~~WICA is located downwind of the Powder River Basin, experiencing a significant decreasing trend in the A4DM8HA at a rate of 1.21 ppbv yr^{-1} ($p = 0.05$) over 2005 – 2014. Curiously, total NO_x emission increased by 29% from 1,327 tons in 2005 to 1,712 tons in 2014 in Custer County, where WICA is located (Table S4). The decreasing A4DM8HA at WICA is attributed to other factors, as discussed in Section 6.~~

~~DINO, RANG, and MEEK are located within the Uintah-Piceance Basin O&NG fields (Figure 1). Increased emissions, most likely from a 68% rise in natural gas production over 2005 – 2015 in the Uintah Basin (Figure 4a), together with snow cover (Edwards et al. 2014; Section xx), could have contributed to very high A4DM8HA O_3 at DINO and RANG. Meanwhile, NO_x emissions from highway vehicles decreased by 86% in Uintah County (Table S4). MEEK, in Rio Blanco County, is located at the eastern edge of the Piceance Basin and relative lower 4DM8HA O_3 (64.1 ppbv) was observed, and trends were not examined for the site's short data record (6 yrs).~~

The four *high*-elevation sites, ROMO, PNDE, CNTL, and GTHC, experienced no trends in their A4DM8HA due likely to opposite changes in emissions from O&NG production, urban sources, and stratospheric intrusion (or a lack thereof). ROMO is located to the west of the

Denver-Julesburg Basin and has experienced northwesterly and southeasterly wind most frequently over 2005 – 2015 (Figure 5a) with higher O_3 (>60 ppbv) from the east and southeast (Figure 5e). Natural gas production in Weld County increased by nearly a factor of 3 from 2009 to 2015, which coincided with use of horizontal drilling starting in 2009 (Figure 4a). Meanwhile ~~the~~a NO_x emission ~~reductions~~reduction of ~37% from the urban area of Denver offset the effect of increased NO_x emissions from O&NG extraction, as evidenced by the significant declines in tropospheric column NO_2 (Figure 4b).

PNDE is located to the north of the Green River Basin, which has two ~~U.S.~~ largest natural gas fields~~,~~ in the U.S., i.e., Pinedale Anticline and Jonah Field. Natural gas production increased steadily over 2005 – 2010 followed by a decline in 2011 and onward. ~~At PNDE, while the~~The dominant winds at PNDE were from the northwest, ~~southeast~~southwest, and northeast (Figure 5b~~),~~). However, O_3 mixing ratios ~~corresponding to~~ in the southwesterly wind, ~~from~~ where expansive O&NG extraction occurred, ~~reached higher than~~can exceed 60 ppbv (Figure 5f). Overall, no trend was observed in natural gas production in Sublette County in the basin (Figure 4a), which was consistent with the relative constant A4DM8HA at PNDE.

CNTL was located to the north of the North Park Basin and southeast of the Green River Basin (Figures 1 and 5g). In the past decade, natural gas production in Jackson County in the North Park Basin decreased by 72% (Figure 4a) and oil production increased comparatively by 73%, which likely contributed to constant A4DM8HA O_3 at CNTL. ~~Similar to all high-elevation sites (i.e., ROMO, PNDE, CNTL),~~ GTHC ~~is another site,~~ located ~~at~~on the mountain ridge~~. The~~, saw high O_3 concentrations from the north (> 65 ppbv) and southwest (> 52 ppbv) ~~indicate that the site was likely under the influence~~indicating combined influences of aforementioned opposite changes in

emissions from the North Park Basin, Denver-Julesburg Basin, and San Juan Basin (Figures 5d and h) ultimately resulting in ~~the site exhibiting~~ no trend in the A4DM8HA.

~~5~~5. Effects of precipitation weather on summertime O_3

We found that summertime O_3 in the Intermountain West was strongly correlated with relative humidity and the wildfire index total fire index (Table S5). Studies have suggested that in the Intermountain West, summertime O_3, especially the seasonal high percentile levels, was impacted by photochemical production from wildfire emissions (Table S5; Jaffe and Wigder, 2012; Lu et al., 2016). To avoid repeating the extensive body of literature on this topic, our own analysis of the effect of wildfires on O_3 can be found in Section S5. One key point coming out of our analysis was, with fire influence removed as indicated in partial correlation, significant negative correlations between summertime O_3 and relative humidity were found at the two reference sites (CRMO and YELL), as well as at the seven O&NG emission influenced sites (CANY CAMP, MEEK, RANG, ROMO, PNDE, and WICA) (Table S5). Further investigation, detailed as follows, revealed that this correlation essentially illuminated the effect of reduced solar radiation on O_3 production caused by cloudiness associated with precipitation weather.

In the Intermountain West, precipitation varies by elevation and latitude among other factors (Williams et al., 1962). The decadal summertime average precipitation abundance was larger at YELL (reference site, 0.17 kg m^{-2}), GTHC, CNTL, ROMO, and WICA (0.15 – 0.27 kg m^{-2}) than that at CRMO (reference site, 0.08 kg m^{-2}) and the remaining sites (Figure 6a). Further examination revealed that YELL, GTHC, CNTL, ROMO, and WICA are located at much higher elevation up in the mountains, where localized convective storms could develop quickly in summer leading to higher precipitation amounts (Williams et al., 1962), and naturally, more cloudiness at these five sites compared to the other sites located at lower elevation within/near the basins. This

is consistent with the significant negative correlations between summertime O_3 and relative humidity at CNTL, ROMO, WICA, and the reference site YELL (Table S5). Note that no significant partial correlation was found between summertime O_3 and relative humidity at GTHC, indicating that summertime O_3 at this site was mostly influenced by wildfire emissions. Significant correlations were also found between solar radiation and summertime median DM8HA O_3 at CNTL (r = 0.67, p = 0.05), ROMO (r = 0.43, p = 0.09), WICA (r = 0.62, p = 0.05), and YELL (r = 0.72, p = 0.01). These results indicate that reduced solar radiation flux near the surface resulting from increased cloudiness accompanying increased precipitation resulted in less O_3 production over the mountain ranges.

Situated on the southern section of the Black Hills, WICA received the highest summertime average precipitation of 0.27 kg m^{-2} (Figure 6a). Total Precipitation showed a significant negative correlation with summertime median DM8HA O_3 at WICA (r = -0.65, p = 0.04, Figure 6b). As noted in Section S5, the decadal highest summertime median DM8HA O_3 was observed in 2012 at 7 sites because of the decadal maximum wild fire emissions. WICA was the exception with its 2012 summertime median DM8HA O_3 being the second largest (58 ppbv) of the decade, compared to the largest value of 61 ppbv in 2006 (Figure 3b), despite the fact that the decadal maximum total fire index occurred in 2012 (0.022 g NO_x m^{-3} in Figure 6b). O_3 levels were expected to be lower in the summer of 2006 because it had the least influence of wildfire emissions evidenced by a very low total fire index value (0.010 g NO_x m^{-3}) (Figure 6b). However, the decadal minimum precipitation (0.18 kg m^{-2}) in the summer of 2006 counteracted the effect of less wildfire emissions (Figure 6b). By comparison, increased cloudiness accompanied more precipitation (0.22 kg m^{-2}) at WICA during the summer of 2012, which dominated over the influence of the decadal maximum wildfire emissions (TFI = 0.021 g NO_x m^{-3}). An increasing trend of 6.7 g m^{-2} yr^{-1} (p = 0.17) was

found in total precipitation at WICA for the time period of 2005 – 2015, indicative of increasing cloudiness. Also, the A4DM8HA values at WICA occurred consistently in late spring/summer, and ultimately the increasing trend in cloudiness linked to increased precipitation likely contributed to the decreasing trend in the A4DM8HA over the decade at this site as shown in the previous section.

Compared to YELL, CNTL, GTHC, ROMO, and WICA, sites located at the lower parts of the basins (i.e., CANY, DINO, MEEK, RANG) had lower annual precipitation levels ranging from 0.08 – 0.12 kg m^{-2} over 2005 – 2015 (Figure 6a). Significant negative correlations were only found between summertime 5th percentile DM8HA O_3 and relative humidity at CANY, MEEK, RANG (Table S5). This indicates that cloudiness associated with precipitation weather had a stronger impact on summertime baseline O_3 than high percentile levels at sites within the basins.

6. Contributions of transport from the Arctic and the West Coast and stratospheric intrusion in winter

Winter seasonal median DM8HA O_3 showed consistent interannual variation with higher O_3 levels (38 – 59 ppbv) in 2011 and 2013 whereas lower values (32 – 44 ppbv) in 2012 at the two references sites and most sites near/within O&NG basins, except the three high-elevation sites ~~(i.e.,~~ GTHC, ROMO, and CNTL~~)~~ (Figures 3c-d). Seasonal 5th and 95th percentile values exhibited similar patterns (not shown). Site and seasonal average O_3 mixing ratios exceeded the decadal average 41 ppbv in 2006, 2008, 2010, 2011, and 2013, and were below average in 2007, 2009, 2012, 2014, and 2015. The difference of the 850 hPa geopotential height between the higher and lower O_3 years is shown in Figure ~~6a~~7a. A pronounced positive difference of ~60 geopotential meters (gpm) was observed over the Arctic polar region and a negative difference of ~ 40 gpm

over the midlatitudes. This pattern ~~strongly~~ indicates a negative (positive) phase of Arctic Oscillation (AO) associated with a higher (lower) O_3 winter in the Intermountain West.

Indeed significant negative correlations (-0.91 to -0.58) were found between the AO index and winter seasonal 50^{th}/95^{th} percentile DM8HA O_3 at most sites, including the reference site YELL over 2005 – 2015 (Table ~~1~~2 and Figure ~~6b~~7b). Significant correlation was not found at the other reference site CRMO, which is located to the south of the Pioneer Mountains and hardly received ~~few~~ air masses (3%) from the north (Figure S1b). Weaker correlations were also observed in the seasonal median DM8HA at CNTL and PNDE. During a longer time period dating back to years prior to 2005, significant negative correlation was observed between seasonal median DM8HA O_3 and the AO index at the reference site YELL (-0.45 over 1997 – ~~2005~~2015), as well as at CANY (-0.47 over 1993 – 2015), CNTL (-0.46 over 1990 – 2015), and ROMO (-0.67 over 1988 – 2015). This ~~indicates~~suggests that the impact of AO on wintertime surface O_3 has been consistently significant during different time periods over the past decades in the Intermountain West.

The negative correlation between AO and wintertime O_3 could be a result of multiple factors, including transport from the Arctic and California, in situ O_3 photochemical production, and stratospheric intrusion. While long-term O_3 trends in lower percentiles could be influenced by long-range transport, O_3 in higher percentiles was more sensitive to local emissions and extreme events (Lin et al., 2017). First, the influence of transport from the Arctic was examined. Artic influence would be foremost demonstrated in surface temperature. During negative AO years, frigid winter air masses could extend far into the middle of North America, contributing to relatively cold temperatures over the U.S. Intermountain West (Hess and Lamarque, 2007). Significant positive correlation was found between the AO index and surface temperature at

CANY, DINO, MEEK, RANG, and GTHC. Except for GTHC, all sites are located within the basins, and weaker positive correlations were observed at other sites, except for CNTL, the highest elevation site in this study (3175 m amsl) (~~Table~~Tables 1 ~~and S1~~ – 2). Significant negative correlation was also found between surface temperature and wintertime O_3 at sites within the basin (i.e., CANY, DINO, MEEK, and RANG), with the potential effect of stratospheric intrusion removed (Partial correlation in Table ~~1~~2). Higher correlation coefficients were found in seasonal 50^{th}/95^{th} DM8HA at DINO, MEEK, and RANG, indicating that the sites were more likely under local influence (Table ~~1~~2). During a colder winter with constant snow cover, high concentrations of O_3 precursors emitted from O&NG extraction were trapped in a shallow boundary layer within the basins followed by strong O_3 photochemical production during daytime leading to the highest O_3 mixing ratios of the season (Schnell et al., 2009; Edwards et al., 2014).

For sites outside the basins that are exposed to distant sources (Figure S1), the significant correlation between wintertime median DM8HA O_3 and the AO index is a strong indication of impacts of long-range transport from source regions afar.

Backward trajectory simulations suggest that long distance transport from the West Coast may obscure the correlation between the AO index and surface O_3 at MEVE, ROMO, YELL, WICA, CNTL, and PNDE. A total of 902 five-day backward trajectories were performed at each site during winters of 2006 – 2015 (Figure ~~7~~8). The difference in numbers of trajectories between high and low O_3 years suggests that more air masses reached the six sites coming from low altitudes (<900 hPa) over the area of southern California and Arizona, centered around 32.5 ºN/120 ºW during high O_3 years (Figure ~~7~~8). At YELL, WICA, PNDE, ROMO, and CNTL, more than 80 backward trajectories passed through the surface of California (Figure ~~7~~8), where ~~large amounts of~~abundant O_3 could be produced from urban emissions ~~of facilities in urban areas~~

(Ryerson et al., 2013). Huang et al. (2013) also found that anthropogenic emissions from southern California could contribute 1 – 15 ppbv to surface O_3 in air masses transported to the Intermountain West. Additionally, more than 20 trajectories originating at YELL, CNTL, ROMO, and MEVE came from higher altitudes (>700 hPa) in the north (>45 °N) during high O_3 years (Figure ~~7~~8). During negative AO (high O_3) years, cold Arctic mid-tropospheric air rich in O_3 would ~~cross Canada~~reach midlatitudes more frequently (Mao and ~~reach~~Talbot, 2004) including the U.S. Intermountain West ~~more frequently ((~~Hess and Lamarque, 2007~~).~~) enhancing surface O_3 there. This is in part evidenced in the significant negative correlation (r = -0.49, p = 0.01) between the AO index and lower tropospheric O_3 at Edmonton, Alberta, Canada over 1988 – 2014 (Figure ~~S2~~S3), indicating stronger impacts of Arctic mid-tropospheric O_3 on the Intermountain West during negative AO years. This also contributes to explaining why the reference site YELL experienced higher seasonal median DM8HA O_3.

Stratospheric influence on surface O_3 was also examined. One of the physical characteristics of stratospheric air is high values of potential vorticity ~~(PV).~~. The differences in ~~PV~~potential vorticity between high and low O_3 years exhibited positive anomalies of ~0.5 ~~PV~~ ~~(10×~~10^{-6} $m^2s^{-1}kg^{-1}K$~~)~~ in the mid-troposphere (315 K) over the Intermountain West (Figure ~~8~~9). Significant negative correlations of -0.64 (p < 0.01) over 1988 – 2015 and -0.76 (p = 0.01) over 2005 – 2015 were found between PV and the AO index over the study region (37.5 °N – 45 °N, -102.5 °W – -110°W). This indicated that stratospheric intrusion over the Intermountain West was associated with the negative AO with a strong impact ~~at~~on sites outside the basins over the region.

~~6. Effects of precipitation weather on summertime O_3~~

We found that summertime O_3 in the Intermountain West was strongly correlated with relative humidity and the wildfire index total fire index (TFI) (Table S6). Studies have suggested that in the Intermountain West, summertime O_3, especially the seasonal high percentile levels, was impacted by photochemical production from wildfire emissions (Table S6; Jaffe and Wigder, 2012; Lu et al., 2016). To avoid repeating the extensive body of literature on this topic, our own analysis of the effect of wildfires on O_3 can be found in Section S7. One key point coming out of our analysis was, with fire influence removed as indicated in partial correlation, significant negative correlations between summertime O_3 and relative humidity were found at the two reference sites (CRMO and YELL), as well as at the 7 O&NG emission influenced sites (CANY CAMP, MEEK, RANG, ROMO, PNDE, and WICA) (Table S6). Further investigation, detailed as follows, revealed that this correlation essentially illuminated the effect of reduced solar radiation on O_3 production caused by cloudiness associated with precipitation weather.

In the Intermountain West, precipitation varies by elevation and latitude among other factors (Williams et al., 1962). The decadal summertime average precipitation abundance was 0.17 kg m^{-2} for the reference site YELL and 0.15 – 0.27 kg m^{-2} for GTHC, CNTL, ROMO, and WICA, which were higher than that at CRMO (0.08 kg m^{-2}) and the remaining sites (Figure 9a). YELL, GTHC, CNTL, ROMO, and WICA are located in the mountains, where localized convective storms could develop quickly in summer leading to higher precipitation amounts (Williams et al., 1962) and naturally, more cloudiness at these five sites compared to the other sites located within the basins. This is consistent with the significant negative correlations between summertime O_3 and relative humidity at CNTL, ROMO, WICA, and the reference site YELL (Table S6). Note that no significant partial correlation was found between summertime O_3 and relative humidity at GTHC, indicating that summertime O_3 at this site was mostly influenced by wildfire emissions.

~~Significant correlations were also found between solar radiation and summertime median DM8HA O_3 at CNTL (r = 0.67, p = 0.05), ROMO (r = 0.43, p = 0.09), WICA (r = 0.62, p = 0.05), and YELL (r = 0.72, p = 0.01). These results indicate that reduced solar radiation flux near the surface resulting from increased cloudiness accompanying increased precipitation resulted in less O_3 production over the mountain ranges.~~

~~Situated on the southern section of the Black Hills, WICA received the highest summertime average precipitation of 0.27 kg m^{-2} (Figure 9a). Total Precipitation showed a significant negative correlation with summertime median DM8HA O_3 at WICA (r = -0.65, p = 0.04, Figure 9b). As noted in Section S7, the decadal highest summertime median DM8HA O_3 was observed in 2012 at 7 sites because of the decadal maximum wild fire emissions. WICA was the exception with its 2012 summertime median DM8HA O_3 being the second largest (58 ppbv) of the decade, compared to the largest value of 61 ppbv in 2006 (Figure 3b), despite the fact that the decadal maximum TFI occurred in 2012 (0.022 g NO_x m^{-3} in Figure 9b). O_3 levels were expected to be lower in the summer of 2006 because it had the least influence of wildfire emissions evidenced by a very low TFI value (0.010 g NO_x m^{-3}) (Figure 9b). However, the decadal minimum precipitation (0.18 kg m^{-2}) in the summer of 2006 counteracted the effect of less wildfire emissions (Figure 9b). By comparison, increased cloudiness accompanied more precipitation (0.22 kg m^{-2}) at WICA during the summer of 2012, which dominated over the influence of the decadal maximum wildfire emissions (TFI = 0.021 g NO_x m^{-3}). An increasing trend of 6.7 g m^{-2} yr^{-1} (p = 0.17) was found in total precipitation at WICA for the time period of 2005 – 2015, indicative of increasing cloudiness and ultimately contributing to the decreasing trend in the A4DM8HA over the decade at this site.~~

~~Compared to YELL, CNTL, GTHC, ROMO, and WICA, sites located at the lower parts of the basins (i.e., CANY, DINO, MEEK, RANG) had lower annual precipitation levels ranging from~~

~~0.08 – 0.12 kg m^{-2} over 2005 – 2015 (Figure 9a). Significant negative correlations were only found between summertime 5th percentile DM8HA O_3 and relative humidity at CANY, MEEK, RANG (Table S6). This indicates a stronger impact of cloudiness associated with precipitation weather on summertime baseline O_3 levels at sites within the basins.~~

7. In situ photochemical O_3 production in winter and summer

To determine the influence of in situ photochemical O_3 production on ambient O_3 in/near O&NG basins, box model simulations were conducted for the Uintah-Piceance Basin, Denver-Julesburg Basin, and its downwind region. In particular, field measurements of VOCs and NO_x in the Uintah Basin during UBWOS 2012 – 2014 were used to understand the role of in situ photochemistry in determining observed O_3 at RANG, DINO, and MEEK during winters of 2012 – 2014 (Figure 1). Measurements during FRAPPÉ at ROMO were used to determine photochemically produced O_3 in summer 2014, while the NACHTT campaign at the Boulder Atmospheric Observatory (BAO) Tower was used for winter 2011. Constraining the model concentrations of VOCs, NO_x, and the radical precursors HCHO, HONO, and $ClNO_2$ using the observed diel profiles reduced the impact of turbulent mixing and transport processes on the in situ photochemical O_3 production. Details of the model simulations can be found in Section S8; Here we focused on discussing the model results in the decadal context. Figure 10 compares the observed average diel cycle of O_3 mixing ratios with those simulated for each campaign. Differences between observed and simulated diel O_3 profiles represent the combined impact of transport processes, stratospheric intrusion, and model uncertainty on surface O_3.

During NACHTT, photochemically produced O_3 at BAO ranged from 6 ppbv at 6:00 am MST to 22 ppbv at 15:00 pm MST, contributing 20 – 52% of the observed O_3 (Figure 10a). Photochemically produced O_3 contributed 30 – 60% of observed O_3 during UBWOS 2012 (Figure

10b). As seen in Figures 10c and 10d, it is possible for the contribution of photochemically produced O_3 during UBWOS 2013 and UBWOS 2014 to exceed the observations. For example, a modeled maximum value of 111 ppbv photochemically produced O_3 was simulated for 16:00 pm MST during UBWOS 2013, larger than the 96 ppbv observed at the site, which indicates that instantaneous mixing with surrounding air and fast transport lowered the photochemically produced O_3 to the observed level.

The decadal highest winter seasonal median DM8HA O_3 was found at DINO (59 ppbv), MEEK (44 ppbv), and RANG (44 ppbv) in winter 2013 (Figure 3c). A positive AO phase ~~was encountered during the~~occurred in winter ~~of~~ 2012 (Figure ~~5b~~6b), where ~~the ambient~~atmospheric conditions were relatively warm without snow cover (Edwards et al., 2013), ~~and the resulting conditions exhibited only~~leading to moderate O_3 production (~31 ppbv in Figure 10b). In contrast to 2012, winter 2013 was in a negative AO phase (Figure ~~6b~~7b), placing the Intermountain West under a strong influence of frigid Arctic air (Section ~~5~~6) and subsequently under meteorologically stagnant conditions and increased snow cover within the basins. As a result, the high levels of VOC emissions from O&NG fields ~~that~~ accumulated in the shallow boundary layer coupled with the increased photolysis rates ~~from the~~due to snow albedo contributed to rapid O_3 production (~78 ppbv in Figure 10c) within the basin, consistent with results from Edward et al. (2014). This result supports the point that surface O_3 at the sites within the basins was attributed mostly to in situ photochemical reactions (Section ~~5~~6).

In contrast to the four wintertime campaigns described above, FRAPPÉ was conducted in the summer. The O_3 measurements from ROMO, located in the center of the FRAPPÉ campaign area, showed a diel cycle with ~40 ppbv nighttime and ~49 ppbv daytime O_3 levels. In contrast, photochemically produced O_3 at ROMO showed a distinct diel cycle with 0 ppbv at night and ~41

ppbv during the day. The strong diel cycle of photochemical production of O_3 at ROMO probably resulted from the combined effect of its high elevation and close proximity to the ~~NFR.~~Colorado Northern Front Range. During the day, large amounts of O_3 precursors from the ~~NFR~~Colorado Northern Front Range transported upward from the southeast (Figure 5a) and contributed to photochemical O_3 production at ROMO (Benedict et al., 2018) followed by dramatically decreased photochemical production accompanied by the collapse of the planetary boundary layer during sunset at ~20:00 MST.

7.1 VOCs-NO_x-O_3 sensitivity

The O_3 sensitivity to NO_x and VOC emissions, which is relevant to the attainment of regional air quality standards, was evaluated in/near O&NG basins. Fifteen simulations for each field campaign were performed with ~~scaled~~ observed VOC and NO_x mixing ratios ~~and,~~ the ~~base case VOC scenario~~latter (NO_x) of which were scaled by a factor varying from 0 to ~~test the sensitivity of daily maximum photochemical O_3 production.~~5. NO_x scaling factor of 1 indicates observed NO_x mixing ratios (Figure 10f). The O_3 formation regime was found be closely associated ~~to~~with the AO phase. Photochemically produced O_3 during UBWOS 2012 and UBWOS 2014 ~~was sensitive to VOCs (Figure 10f),~~decreased with increasing NO_x mixing ratios, indicating ~~that~~VOC-limited O_3 formation regimes (Figure 10f). Therefore, O_3 photochemistry at DINO, RANG, and MEEK was also likely to be radical limited in winter 2012 and 2014. In contrast to these two winters, O_3 photochemistry had mixed sensitivity during UBWOS 2013 (Figure 10f), when in situ photochemically produced O_3 could be as high as 111 ppbv. Winter 2013 was in a negative AO phase, while winters of 2012 and 2014 were in positive phases. As ~~stated in Section 5~~aforementioned, surface O_3 at the sites within the basin was attributed mostly to in situ photochemical reactions. Therefore, for areas within the basins, emission reductions in VOCs

alone would lead to O_3 mitigation in positive AO years, while emission reductions in both VOCs and NO_x would be effective in negative AO years. In the ~~NFR~~Colorado Northern Front Range region, photochemical O_3 production in winter 2011 surrounding BAO was sensitive to VOCs during NACHTT (Figure 10f). Photochemical O_3 production at ROMO in summer 2014 had mixed sensitivity (Figure 10f).

Edwards et al. (2013) also simulated an average UBWOS 2012 day (15 January to 1 March 2012) and found the same O_3 formation regime as our study. They found that the radical-limited O_3 photochemistry in 2012 was driven by the very low radical production rates (~2.3 ppbv day^{-1}) in comparison to the emission rate of NO_x. While an average UBWOS 2013 day (23 January to 24 March 2013) was simulated in our study, Edwards et al. (2014) simulated a single stagnant six-day (31 January to 5 February 2013) ~~strong~~high O_3 event, when DM8HA O_3 increased from 67 to 107 ppbv. ~~It was~~They found that O_3 in winter 2013 was sensitive to changes of NO_x, and the total net radical production rate could be as high as ~19 ppbv day^{-1}, which was sufficient to prevent NO_x saturation ~~(Edward et al., 2014).~~.

8. Summary

~~Our study suggested that decadal~~Two reference sites, YELL and CRMO, exhibited no significant trends in the A4DM8HA O_3 over ~~the Intermountain West during~~ 2005 – 2015. Our analysis suggested that, without the immediate influence of O&NG emissions, the lack of trend and the interannual variation at the two reference sites were ~~shaped~~driven by precipitation weather, wildfire emissions, stratospheric intrusion, and transport from the Arctic and the West Coast facilitated by regional to hemispheric circulation. ~~Trends over the areas~~In contrast, decadal trends at sites near/within O&NG basins were predominantly impacted by changes in emissions from the O&NG basins among other anthropogenic sources. ~~Two reference sites, YELL and CRMO,~~

~~exhibited no significant trends in the A4DM8HA O_3 over 2005 – 2015, indicating, without the immediate influence of O&NG emissions, relatively constant O_3 levels over the Intermountain West. In contrast, decadal trends in the A4DM8HA varied at the 11 sites located either in or near the O&NG extraction basins. A significant decreasing trend of -0.76~~ A significant decreasing trend of -0.83 ppbv yr^{-1} at MEVE was associated with the decreasing natural gas production (37%) in the San Juan Basin, while ~~a significant decreasing trend (-~~that of -0.~~54~~58 ppbv yr^{-1}~~)~~ at CANY was predominately influenced by declining extraction of CBM in the Paradox Basin and emission reductions of 35% in electricity generation from coal. Increasing precipitation (6.7 g m^{-2} yr^{-1}) resulting from increasing cloudiness ~~in the southern portion of the Black Hills~~ contributed to the decreasing trend in the A4DM8HA (-1.~~21~~16 ppbv yr^{-1}) at WICA. No trends were found ~~in the 4DM8HA~~ at the remaining sites, resulting likely from the combined effect of increasing emissions from O&NG extraction and decreasing emissions from other sectors.

In winter, seasonal 50^{th}/95^{th} DM8HA O_3 was associated with the AO at 8 sites, including the reference site YELL. For sites within the O&NG basins, O&NG emissions, colder surface air temperature, and enhanced solar radiation due to snow cover contributed to higher O_3, especially in the seasonal 95^{th} levels during negative AO years, and emission reductions in both VOCs and NO_x could lead to effective O_3 mitigation. For sites outside the O&NG basins, the ~~high O_3 in~~higher seasonal 50^{th} percentile DM8HA O_3 levels were a result of transport from the Arctic or California ~~and~~together with stratospheric intrusion. In summer, the interannual variation of O_3 was predominantly affected by precipitation weather at 9 sites including the two reference sites. At high-elevation sites in the mountains, more abundant precipitation (0.18 – 0.27 kg m^{-2}) induced more cloudiness and consequently reduced solar flux leading less O_3 production in seasonal 5^{th}/50^{th}/95^{th} levels. However, at sites within the basin, the cloudiness associated with precipitation

weather had a stronger impact on summertime baseline O_3 levels (i.e., the 5th percentile).

~~This study is the first one to investigate the long term impact of O&NG extraction activities on the distribution and trend of surface O_3 over the intermountain U.S.~~To the best of our knowledge, only two studies investigated the long-term impact of O&NG extraction on the trend of surface O_3 and its precursors (Majid et al., 2017; Bien and Helmig, 2018). Majid et al. (2017) investigated the decadal trends in OMI-retrieved NO_2 in 7 main shale plays over 2005 – 2015 and found O&NG industry was reversing the rate of changes in NO_2. Bien and Helmig (2018) found surface O_3 at sites within O&NG production basins can be ranked among top ten of all Colorado sites, and further suggested the need of more continuous measurements within O&NG basins to study the long-term influence of O&NG emissions. O&NG activities have varied greatly over the past decade. In Wyoming, annual O&NG production levels have fallen significantly in the Jonah Field since 2009 and the Pinedale Field since 2012, because of lower natural gas prices relative to crude oil (http://wogcc.wyo.gov/). In Colorado, the number of active wells in Weld County increased by ~2000 between 2012 and 2014, followed by a decline since early 2015 (http://cogcc.state.co.us/data.html). However, current emission inventories underestimated VOC emissions from O&NG productions by a factor of 2 or more (Pétron et al., 2014). While data analysis studies provided measurement-based estimates of contributions from various processes to decadal variability of surface O_3, we understand their limitation in clearly separating such contributions. Detailed multiyear studies that integrate measurements and three-dimensional chemical transport model simulations with accurate emission inventories are needed to further quantify the contribution of each process identified in this work.

Author Contributions

YZ and HM designed this study. BS provided long-term surface observations. YZ led the analysis

and writing of this manuscript ~~with~~, HM contributed to manuscript writing, and BS contributed significant ~~contributions~~scientific and editorial comments ~~from HM and BS~~.

Acknowledgements

This work was supported by the Chemistry Emeriti Faulty Award from the Department of Chemistry at SUNY College of Environmental Science and Forestry and the National Park Service. We are grateful to Jessica Ward, Air Resources Specialists, Inc. for retrieving and providing the National Park Service data. We thank Cara Kesler for providing data from the Wyoming Department of Environmental Quality. We acknowledge the free use of tropospheric NO_2 column data from the OMI sensor from www.temis.nl. We thank the two anonymous reviewers for their constructive comments and suggestions. The assumptions, findings, conclusions, judgements, and views presented herein are those of the authors and should not be interpreted as necessarily representing the National Park Service.

References

Abeleira, A. J. and Farmer, D. K.: Summer ozone in the northern Front Range metropolitan area: weekend–weekday effects, temperature dependences, and the impact of drought. Atmos. Chem. Phys., 17, 6517-6529, https://doi.org/10.5194/acp-17-6517-2017, 2017.

Akagi, S. K., Yokelson, R. J., Wiedinmyer, C., Alvarado, M. J., Reid, J. S., Karl, T., Crounse, J. D., and Wennberg, P. O.: Emission factors for open and domestic biomass burning for use in atmospheric models. Atmos. Chem. Phys., 11, 4039-4072, https://doi.org/10.5194/acp-11-4039-2011, 2011.

Allen, D.T.: Atmospheric emissions and air quality impacts from natural gas production and use, Annu. Rev. Chem. Biomol. Eng. 5, 55-75, doi:10.1146/annurev-chembioeng-060713-035938, 2014.

Allen, D. T.: Emissions from oil and gas operations in the United States and their air quality implications, Journal of the Air & Waste Management Association, 66:6,549-575, DOI: 10.1080/10962247.2016.1171263, 2016.

Benedict, K. B., Zhou, Y., Sive, B. C., Prenni, A. J., Gebhart, K. A., Fischer, E. V., Evanoski-Cole, A., Sullivan, A. P., Callahan, S., Schichtel, B. A., Mao, H., Zhou, Y., and Collett Jr., J. L.: Volatile organic compounds and ozone in Rocky Mountain National Park during FRAPPÉ, Atmos. Chem. Phys., 19, 499-521, https://doi.org/10.5194/acp-19-499-2019, 2019.

Bien, T. and Helmig, D.: Changes in summertime ozone in Colorado during 2000–2015. Elem Sci

Anth, 6(1), p.55. DOI: http://doi.org/10.1525/elementa.300, 2018.

Carter, W. P. L. and Seinfeld, J. H.: Winter ozone formation and VOC incremental reactivities in the Upper Green River Basin of Wyoming. Atmospheric Environment, 50, 255-266, https://doi.org/10.1016/j.atmosenv.2011.12.025, 2012

Chan, E.: Regional ground-level ozone trends in the context of meteorological influences across Canada and the eastern United States from 1997 to 2006. Journal of Geophysical Research: Atmospheres, 114, 1-18, https://doi.org/10.1029/2008JD010090, 2009.

Cheadle, L.C., Oltmans, S.J., Petron, G., Schnell, R.C., Mattson, E.J., Herndon, S.C., Thompson, A.M., Blake, D.R. and McClure-Begley, A., 2017. Surface ozone in the Colorado northern Front Range and the influence of oil and gas development during FRAPPE/DISCOVER-AQ in summer 2014. Elem Sci Anth, 5, p.61. DOI: http://doi.org/10.1525/elementa.254

Cooper, O. R., Gao, R. S., Tarasick, D., Leblanc, T., and Sweeney, C.: Long-term ozone trends at rural ozone monitoring sites across the United States, 1990-2010. Journal of Geophysical Research: Atmospheres, 117, 1990-2010, https://doi.org/10.1029/2012JD018261, 2012.

Cooper, O.R., Parrish, D.D., Ziemke, J., Balashov, N.V., Cupeiro, M., Galbally, I.E., Gilge, S., Horowitz, L., Jensen, N.R., Lamarque, J.-F., Naik, V., Oltmans, S.J., Schwab, J., Shindell, D.T., Thompson, A.M., Thouret, V., Wang, Y. and Zbinden, R.M.: Global distribution and trends of tropospheric ozone: An observation-based review. Elem Sci Anth, 2, p.000029. DOI:http://doi.org/10.12952/journal.elementa.000029, 2014.

Draxler, R. R., and Hess, G. D.: NOAA Technical Memorandum ERL ARL-224, 28. https://www.arl.noaa.gov/documents/reports/arl-224.pdf, 1998.

Edwards, P. M., Young, C. J., Aikin, K., deGouw, J., Dubé, W. P., Geiger, F., Gilman, J., Helmig, D., Holloway, J. S., Kercher, J., Lerner, B., Martin, R., McLaren, R., Parrish, D. D., Peischl, J., Roberts, J. M., Ryerson, T. B., Thornton, J., Warneke, C., Williams, E. J., and Brown, S. S.: Ozone photochemistry in an oil and natural gas extraction region during winter: simulations of a snow-free season in the Uintah Basin, Utah, Atmos. Chem. Phys., 13, 8955-8971, https://doi.org/10.5194/acp-13-8955-2013, 2013.

Edwards, P.M., Brown, S.S., Roberts, J.M., Ahmadov, R., Banta, R.M., DeGouw, J. A., Dubé, W.P., Field, R. A., Flynn, J.H., Gilman, J.B., Graus, M., Helmig, D., Koss, A., Langford, A.O., Lefer, B.L., Lerner, B.M., Li, R., Li, S.-M., McKeen, S. A., Murphy, S.M., Parrish, D.D., Senff, C.J., Soltis, J., Stutz, J., Sweeney, C., Thompson, C.R., Trainer, M.K., Tsai, C., Veres, P.R., Washenfelder, R. a., Warneke, C., Wild, R.J., Young, C.J., Yuan, B., Zamora, R: High winter ozone pollution from carbonyl photolysis in an oil and gas basin. Nature, 514(7522), 351-354, https://doi.org/10.1038/nature13767, 2014.

Energy Information Administration (EIA): Shale in the United States. Retrieved from http://www.eia.gov/energy_in_brief/article/shale_in_the_united_states.cfm, 2015.

Environmental Protection Agency (EPA): Regulatory Actions | Ground-level Ozone | US EPA. Retrieved February 8, 2016, from http://www3.epa.gov/ozonepollution/actions.html, 2015.

Helmig, D., Thompson, C. R., Evans, J., Boylan, P., Hueber, J., and Park, J.-H.: Highly elevated atmospheric levels of volatile organic compounds in the Uintah Basin, Utah. Environmental Science & Technology, 48, 4707-4715, https://doi.org/10.1021/es405046r, 2014.

Gaudel, A., Cooper, O.R., Ancellet, G., Barret, B., Boynard, A., Burrows, J.P., Clerbaux, C., Coheur, P.-F., Cuesta, J., Cuevas, E., Doniki, S., Dufour, G., Ebojie, F., Foret, G., Garcia, O., Granados Muñoz, M.J., Hannigan, J.W., Hase, F., Huang, G., Hassler, B., Hurtmans, D., Jaffe, D., Jones, N., Kalabokas, P., Kerridge, B., Kulawik, S.S., Latter, B., Leblanc, T., Le Flochmoën, E., Lin, W., Liu, J., Liu, X., Mahieu, E., McClure-Begley, A., Neu, J.L., Osman, M., Palm, M., Petetin, H., Petropavlovskikh, I., Querel, R., Rahpoe, N., Rozanov, A., Schultz, M.G., Schwab, J., Siddans, R., Smale, D., Steinbacher, M., Tanimoto, H., Tarasick, D.W., Thouret, V., Thompson, A.M., Trickl, T., Weatherhead, E., Wespes, C., Worden, H.M., Vigouroux, C., Xu, X., Zeng, G. and Ziemke, J.: Tropospheric Ozone Assessment Report: Present-day distribution and trends of tropospheric ozone relevant to climate and global atmospheric chemistry model evaluation. Elem Sci Anth, 6, p.39, http://doi.org/10.1525/elementa.291, 2018.

Hess, P. G. and Lamarque, J. F.: Ozone source attribution and its modulation by the Arctic oscillation during the spring months. Journal of Geophysical Research: Atmospheres, 112, 1-17, https://doi.org/10.1029/2006JD007557, 2007.

Huang, M., Bowman, K. W., Carmichael, G. R., Bradley, P. R., Worden, H. M., Luo, M., Cooper, O. R., Pollack, I. B., Ryerson, T. B., Brown, S. S.: Impact of Southern California anthropogenic emissions on ozone pollution in the mountain states: Model analysis and observational evidence from space. Journal of Geophysical Research: Atmospheres, 118, 12,784-12,803, https://doi.org/10.1002/2013JD020205, 2013.

Jaffe, D., Chand, D., Hafner, W., Westerling, A., and Spracklen, D.: Influence of Fires on O3 Concentrations in the Western U.S. Environmental Science & Technology, 42, 5885-5891, https://doi.org/10.1021/es800084k, 2008.

Jaffe, D. A. and Wigder, N. L.: Ozone production from wildfires: A critical review. Atmospheric Environment, 51, 1-10, https://doi.org/10.1016/j.atmosenv.2011.11.063, 2012.

Jenkin, M. E., Young, J. C., and Rickard, A. R.: The MCM v3.3.1 degradation scheme for isoprene. Atmos. Chem. Phys., 15, 11433-11459, https://doi.org/10.5194/acp-15-11433-2015, 2015.

Karion, A., Sweeney, C., Petron, G., Frost, G., Hardesty, R. M., Kofler, J., Miller, B. R., Newberger, T., Wolter, S., Banta, R., Brewer, A., Dlugokencky, E., Lang, P., Montzka, S. A., Schnell, R., Tans, P., Trainer, M., Zamora, R., Conley, S.: Methane emissions estimate from airborne measurements over a western United States natural gas field Geophys. Res. Lett., 40, 4393-4397, DOI: 10.1002/grl.50811, 2013.

Knote, C., Tuccella, P., Curci, G., Emmons, L., Orlando, J.J., Madronich, S., Baró, R., Jiménez-Guerrero, P., Luecken, D., Hogrefe, C., Forkel, R., Werhahn, J., Hirtl, M., Pérez, J.L., San José, R., Giordano, L., Brunner, D., Yahya, K., Zhang, Y.: Influence of the choice of gas-phase mechanism on predictions of key gaseous pollutants during the AQMEII phase-2 intercomparison. Atmospheric Environment, 115, 553-568, https://doi.org/10.1016/j.atmosen v.2014.11.066, 2015.

Lin, M., Horowitz, L. W., Payton, R., Fiore, A. M., and Tonnesen, G.: US surface ozone trends and extremes from 1980 to 2014: quantifying the roles of rising Asian emissions, domestic controls, wildfires, and climate. Atmos. Chem. Phys., 17, 2943-2970, https://doi.org/10.51 94/acp-17-2943-2017, 2017.

Lin, M., Horowitz, L. W., Oltmans, S. J., Fiore, A. M., and Fan, S.: Tropospheric ozone trends at Mauna Loa Observatory tied to decadal climate variability. Nature Geoscience, 7, 136-143, https://doi.org/10.1038/ngeo2066, 2014.

Lu, X., Zhang, L., Yue, X., Zhang, J., Jaffe, D. A., Stohl, A., Zhao, Y., and Shao, J.: Wildfire influences on the variability and trend of summer surface ozone in the mountainous western United States, Atmos. Chem. Phys., 16, 14687-14702, https://doi.org/10.5194/acp-16-14687-2016, 2016.

Madronich, S., McKenzie, R. L., Björn, L. O., and Caldwell, M. M.: Changes in biologically active ultraviolet radiation reaching the Earth's surface. Journal of Photochemistry and Photobiology B: Biology, 46, 5-19, https://doi.org/10.1016/S1011-1344(98)00182-1, 1998.

Mao, H., and Talbot, R.: Relationship of surface O_3 to large-scale circulation patterns during two recent winters, Geophys. Res. Lett., 31(6), L06108, 10.1029/2003GL018860, 2004.

Natural Gas Intelligence (NGI): Major & Minor Resource Plays. Retrieved April 27, 2018, from http://www.naturalgasintel.com/Major-and-Minor-North-American-Shale-Basins-and-Resource-Plays, 2018.

McDuffie, E. E., Edwards, P. M., Gilman, J. B., Lerner, B. M., Dubé, W. P., Trainer, M., Wolfe, D. E., Angevine, W. M., deGouw, J., Williams, E. J., Tevlin, A. G., Murphy, J. G., Fischer, E. V., McKeen, S., Ryerson, T. B., Peischl, J., Holloway, J. S., Aikin, K., Langford, A. O., Senff, C. J., Alvarez, R. J., Hall, S. R., Ullmann, K., Lantz, K. O., Brown, S. S.: Influence of oil and gas emissions on summertime ozone in the Colorado Northern Front Range. Journal of Geophysical Research: Atmospheres, 121, 8712-8729, https://doi.org/10.1002/2016JD025265, 2016.

Monks, P.S., Granier, C., Fuzzi, S., Stohl, A., Williams, M.L., Akimoto, H., Amann, M., Baklanov, A., Baltensperger, U., Bey, I., Blake, N., Blake, R.S., Carslaw, K., Cooper, O.R., Dentener, F., Fowler, D., Fragkou, E., Frost, G.J., Generoso, S., Ginoux, P., Grewe, V., Guenther, A., Hansson, H.C., Henne, S., Hjorth, J., Hofzumahaus, A., Huntrieser, H., Isaksen, I.S.A., Jenkin, M.E., Kaiser, J., Kanakidou, M., Klimont, Z., Kulmala, M., Laj, P., Lawrence, M.G., Lee, J.D., Liousse, C., Maione, M., McFiggans, G., Metzger, A., Mieville, A., Moussiopoulos, N., Orlando, J.J., O'Dowd, C.D., Palmer, P.I., Parrish, D.D., Petzold, A., Platt, U., Pöschl, U., Prévôt, A.S.H., Reeves, C.E., Reimann, S., Rudich, Y., Sellegri, K., Steinbrecher, R., Simpson, D., ten Brink, H., Theloke, J., van der Werf, G.R., Vautard, R., Vestreng, V., Vlachokostas, C., von Glasow, R.: Atmospheric composition change – global and regional air quality. Atmospheric Environment, 43, 5268-5350, https://doi.org/10.1016/j.atmosenv.2009.08.021, 2009.

Oltmans, S.J., Cheadle, L.C., Johnson, B.J., Schnell, R.C., Helmig, D., Thompson, A.M., Cullis, P., Hall, E., Jordan, A., Sterling, C., McClure-Begley, A., Sullivan, J.T., McGee, T.J. and Wolfe, D., 2019. Boundary layer ozone in the Northern Colorado Front Range in July–August 2014 during FRAPPE and DISCOVER-AQ from vertical profile measurements. Elem Sci Anth, 7(1), p.6. DOI: http://doi.org/10.1525/elementa.345

Parrish, D.D., Law, K.S., Staehelin, J., Derwent, R., Cooper, O.R., Tanimoto, H., Volz-Thomas, A., Gilge, S., Scheel, H.E., Steinbacher, M., Chan, E.: Long-term changes in lower tropospheric baseline ozone concentrations at northern mid-latitudes. Atmos. Chem. Phys., 12, 11485-11504, https://doi.org/10.5194/acp-12-11485-2012, 2012.

Parrish, D.D., Law, K.S., Staehelin, J., Derwent, R., Cooper, O.R., Tanimoto, H., Volz-Thomas, A., Gilge, S., Scheel, H.E., Steinbacher, M., Chan, E.: Lower tropospheric ozone at northern midlatitudes: Changing seasonal cycle. Geophysical Research Letters, 40, 1631-1636, https://doi.org/10.1002/grl.50303, 2013.

Péron, G., Karion, A., Sweeney, C., Miller, B.R., Montzka, S.A., Frost, G.J., Trainer, M., Tans, P., Andrews, A., Kofler, J., Helmig, D., Guenther, D., Dlugokencky, E., Lang, P., Newberger, T.,

Wolter, S., Hall, B., Novelli, P., Brewer, A., Conley, S., Hardesty, M., Banta, R., White, A., Noone, D., Wolfe, D., Schnell, R.: A new look at methane and nonmethane hydrocarbon emissions from oil and natural gas operations in the Colorado Denver-Julesburg Basin. Journal of Geophysical Research: Atmospheres, 119, 6836-6852, https://doi.org/10.1002/2013JD021272, 2014.

Pfister G. G., Reddy P. J., Barth M. C., Flocke F. F., Fried A., Herndon S. C., Sive B. C., Sullivan J. T., Thompson A. M., Yacovitch T. I., Weinheimer A. J., Wisthaler A.: Using Observations and Source - Specific Model Tracers to Characterize Pollutant Transport During FRAPPÉ and DISCOVER - AQ. Journal of Geophysical Research: Atmospheres, 122, 10,510-10,538, https://doi.org/10.1002/2017JD027257, 2007.

Rappenglück, B., Ackermann, L., Alvarez, S., Golovko, J., Buhr, M., Field, R. A., Soltis, J., Montague, D. C., Hauze, B., Adamson, S., Risch, D., Wilkerson, G., Bush, D., Stoeckenius, T., and Keslar, C.: Strong wintertime ozone events in the Upper Green River basin, Wyoming, Atmos. Chem. Phys., 14, 4909-4934, https://doi.org/10.5194/acp-14-4909-2014, 2014.

Reddy, P. J. and Pfister, G. G.: Meteorological factors contributing to the interannual variability of midsummer surface ozone in Colorado, Utah, and other western U.S. states. Journal of Geophysical Research: Atmospheres, 121, 2434-2456, https://doi.org/10.1002/2015JD023840, 2016.

Reidmiller, D. R., Fiore, A. M., Jaffe, D. A., Bergmann, D., Cuvelier, C., Dentener, F. J., Duncan, B. N., Folberth, G., Gauss, M., Gong, S., Hess, P., Jonson, J. E., Keating, T., Lupu, A., Marmer, E., Park, R., Schultz, M. G., Shindell, D. T., Szopa, S., Vivanco, M. G., Wild, O., and Zuber, A.: The influence of foreign vs. North American emissions on surface ozone in the US, Atmos. Chem. Phys., 9, 5027-5042, https://doi.org/10.5194/acp-9-5027-2009, 2009.

Rodriguez, M. A., Barna, M. G., and Moore, T.: Regional Impacts of Oil and Gas Development on Ozone Formation in the Western United States. Journal of the Air & Waste Management Association, 59, 1111-1118, https://doi.org/10.3155/1047-3289.59.9.1111, 2009.

Ryerson T. B., Andrews A. E., Angevine W. M., Bates T. S., Brock C. A., Cairns B., Cohen R. C., Cooper O. R., Gouw J. A., Fehsenfeld F. C., Ferrare R. A., Fischer M. L., Flagan R. C., Goldstein A. H., Hair J. W., Hardesty R. M., Hostetler C. A., Jimenez J. L., Langford A. O., McCauley E., McKeen S. A., Molina L. T., Nenes A., Oltmans S. J., Parrish D. D., Pederson J. R., Pierce R. B., Prather K., Quinn P. K., Seinfeld J. H., Senff C. J., Sorooshian A., Stutz J., Surratt J. D., Trainer M., Volkamer R., Williams E. J., Wofsy S. C.: The 2010 California Research at the Nexus of Air Quality and Climate Change (CalNex) field study. Journal of Geophysical Research: Atmospheres, 118, 5830-5866, https://doi.org/10.1002/jgrd.50331, 2013.

Schnell, R. C., Oltmans, S. J., Neely, R. R., Endres, M. S., Molenar, J. V., and White, A. B.: Rapid photochemical production of ozone at high concentrations in a rural site during winter. Nature Geoscience, 2, 120-122, https://doi.org/10.1038/ngeo415, 2009.

Stohl A., Bonasoni P., Cristofanelli P., Collins W., Feichter J., Frank A., Forster C., Gerasopoulos E., Gäggeler H., James P., Kentarchos T., Kromp-Kolb H., Krüger B., Land C., Meloen J., Papayannis A., Priller A., Seibert P., Sprenger M., Roelofs G. J., Scheel H. E., Schnabel C., Siegmund P., Tobler L., Trickl T., Wernli H., Wirth V., Zanis P., Zerefos C.: Stratosphere - troposphere exchange: A review, and what we have learned from STACCATO. Journal of Geophysical Research: Atmospheres, 108, https://doi.org/10.1029/2002JD002490, 2003.

Swarthout, R. F., Russo, R. S., Zhou, Y., Hart, A. H., and Sive, B. C.: Volatile organic compound distributions during the NACHTT campaign at the Boulder Atmospheric Observatory: Influence of urban and natural gas sources. Journal of Geophysical Research: Atmospheres, 118, 10,614-10,637, https://doi.org/10.1002/jgrd.50722, 2013.

Thompson, T. M., D. Shepherd, A. Stacy, M. G. Barna, and B. A. Schichtel: Modeling to Evaluate Contribution of Oil and Gas Emissions to Air Pollution, Journal of the Air & Waste Management Association, 67, 445-461, DOI:10.1080/10962247.2016.1251508, 2017.

Westerling, A. L., Hidalgo, H. G., Cayan, D. R., and Swetnam, T. W.: Warming and Earlier Spring Increase Western U.S. Forest Wildfire Activity. Science, 313, 940-943, https://doi.org/10.1126/science.1128834, 2006.

Williams, P. and Peck, E. L.: Terrain Influences on Precipitation in the Intermountain West as Related to Synoptic Situations. Journal of Applied Meteorology, 1, 343-347, https://doi.org/10.1175/1520-0450(1962)001<0343:TIOPIT>2.0.CO;2, 1962.

Zhou, Y., Mao, H., Demerjian, K., Hogrefe, C., and Liu, J.: Regional and hemispheric influences on temporal variability in baseline carbon monoxide and ozone over the Northeast US. Atmospheric Environment, 164, 309-324, https://doi.org/10.1016/j.atmosenv.2017.06.017, 2017.

Table 1. Names and locations of sites used in this study. Gray and blue shades indicate sites located outside of 100 km of shale plays. CRMO and YELL in blue shades are located upwind of O&NG extraction fields and used as reference sites.

Site Abbreviation	Park Unit/Measurement Network	Site	Latitude	Longitude	Elevation (m)	Start Date	End Date	Year-round Measurement
CANY	Canyonlands National Park	Island in the Sky	38.46	-109.82	1809	7/1/1992	12/30/2015	1993 - 2015
DINO	Dinosaur National Monument	West Entrance Housing	40.29	-108.94	1463	4/1/2005	12/30/2015	2011 - 2015
MEEK	Meeker	Plant Science Resource Management	40.00	-107.85	1994	1/1/2010	12/30/2015	2010 - 2015
MEVE	Mesa Verde National Park	Area	37.20	-108.49	2165	3/1/1993	12/30/2015	1995 - 2015
RANG	Rangely	Golf Course	40.09	-108.76	1655	8/1/2010	12/30/2015	2011 - 2015
ROMO	Rocky Mountain National Park	Long's Peak	40.28	-105.55	2743	4/1/1987	12/30/2015	1998 - 2015
WICA	Wind Cave National Park	Visitor Center	43.56	-103.48	1292	12/31/2003	12/30/2015	2005 - 2008; 2010 - 2014
CAMP	Wyoming Department of Environmental Quality	Campbell, WY	44.15	-105.53	1427	1/1/2005	12/31/2015	2005 - 2015
CNTL	Clean Air Status and Trends Network	Centennial, WY	41.36	-106.24	3175	5/9/1989	12/31/2015	1990 - 2015
GTHC	Clean Air Status and Trends Network	Gothic, CO	38.96	-106.99	2915	5/13/1989	12/31/2015	1990 - 2015
PNDE	Clean Air Status and Trends Network	Pinedale, WY	42.93	-109.79	2386	10/21/1988	12/31/2015	1989 - 1994; 1996 - 2015
BADL	Badlands National Park	Visitor Center	43.74	-101.94	739	10/1/1987	12/31/2014	1988 - 1991; 2004 - 2014
CRMO	Craters of the Moon National Monument & Preserve	Visitor Center	43.46	-113.56	1815	9/24/1992	12/30/2015	1993 - 2004; 2007 - 2015
GRBA	Great Basin National Park	Maintenance Yard	39.01	-114.22	2060	8/24/1993	12/30/2015	1994 - 2015
GRCA	Grand Canyon National Park	The Abyss	36.06	-112.18	2073	1/1/1993	12/30/2015	1993 - 2015
PEFO	Petrified Forest National Park	South Entrance	34.82	-109.89	1723	1/1/2002	12/30/2015	2003 - 2015
YELL	Yellowstone National Park	Water Tank	44.56	-110.40	2400	6/1/1996	12/30/2015	1997 - 2015
ZION	Zion National Park	Dalton's Wash	37.20	-113.15	1213	1/1/2004	12/30/2015	2004 - 2015

* MEEK and RANG are not located in national parks, but measurements at these two sites are also maintained by the National Park Service.

Table 2. Correlation coefficients (r) and p-value in parenthesis between the pairs of variables in winter over 2006 – 2015. Partial correlation was computed for surface temperature and seasonal 95th DM8HA by controlling the effect of PV. Boldfaced numbers indicate p-value ≤ 0.10.

		r (O_3 vs AO)				r (O_3 vs Temperature)			Partial r
Site	Time Period	5th	50th	95th	r (AO vs temperature)	5th	50th	95th	95th
CANY	2006 - 2015	**-0.63 (0.05)**	**-0.72 (0.02)**	**-0.73 (0.02)**	**0.66 (0.04)**	**-0.81 (<0.01)**	**-0.64 (0.05)**	**-0.64 (0.04)**	**-0.62 (0.06)**
CAMP	2006 - 2015	0.06 (0.88)	-0.15 (0.67)	-0.30 (0.40)	0.31 (0.38)	0.11 (0.75)	-0.36 (0.31)	-0.21 (0.55)	-0.27 (0.49)
DINO	2011 - 2015	-0.29 (0.64)	**-0.89 (0.04)**	**-0.94 (0.02)**	**0.90 (0.04)**	-0.53 (0.36)	**-0.94 (0.02)**	**-0.96 (0.01)**	**-0.95 (0.05)**
MEEK	2011 - 2015	**-0.88 (0.02)**	**-0.91 (0.01)**	**-0.92 (0.01)**	**0.93 (0.02)**	**-0.84 (0.07)**	**-0.91 (0.03)**	**-0.85 (0.06)**	**-0.96 (0.04)**
RANG	2011 - 2015	-0.05 (0.93)	**-0.91 (0.03)**	**-0.93 (0.02)**	**0.92 (0.03)**	-0.38 (0.53)	**-0.99 (<0.01)**	**-0.95 (0.01)**	**-0.92 (0.08)**
MEVE	2006 - 2015	-0.53 (0.11)	**-0.70 (0.02)**	**-0.64 (0.04)**	0.53 (0.12)	**-0.54 (0.10)**	**-0.63 (0.05)**	**-0.59 (0.07)**	-0.28 (0.47)
ROMO	2006 - 2015	-0.09 (0.81)	**-0.72 (0.01)**	-0.49 (0.15)	0.50 (0.14)	-0.36 (0.31)	-0.48 (0.16)	-0.21 (0.56)	-0.14 (0.72)
WICA	2006 - 2014	0.25 (0.52)	**-0.58 (0.10)**	-0.39 (0.21)	0.26 (0.46)	-0.28 (0.51)	-0.50 (0.21)	-0.50 (0.20)	-0.49 (0.26)
CNTL	2006 - 2015	-0.04 (0.91)	-0.47 (0.17)	-0.38 (0.28)	-0.32 (0.37)	**0.63 (0.05)**	**0.73 (0.02)**	**0.66 (0.04)**	**0.66 (0.05)**
GTHC	2006 - 2015	-0.15 (0.67)	-0.03 (0.93)	0.04 (0.92)	**0.58 (0.08)**	-0.35 (0.32)	-0.23 (0.52)	-0.44 (0.20)	-0.55 (0.12)
PNDE	2006 - 2015	-0.29 (0.42)	-0.46 (0.18)	-0.05 (0.89)	0.30 (0.40)	-0.27 (0.45)	-0.09 (0.80)	-0.43 (0.21)	**-0.63 (0.07)**
CRMO	2008 - 2015	-0.41 (0.31)	-0.28 (0.51)	-0.10 (0.82)	0.53 (0.11)	-0.54 (0.16)	**-0.72 (0.04)**	-0.55 (0.16)	**-0.85 (0.01)**
YELL	2006 - 2015	**-0.68 (0.03)**	**-0.77 (<0.01)**	-0.46 (0.19)	0.37 (0.15)	**-0.63 (0.05)**	-0.43 (0.22)	-0.43 (0.22)	-0.37 (0.32)

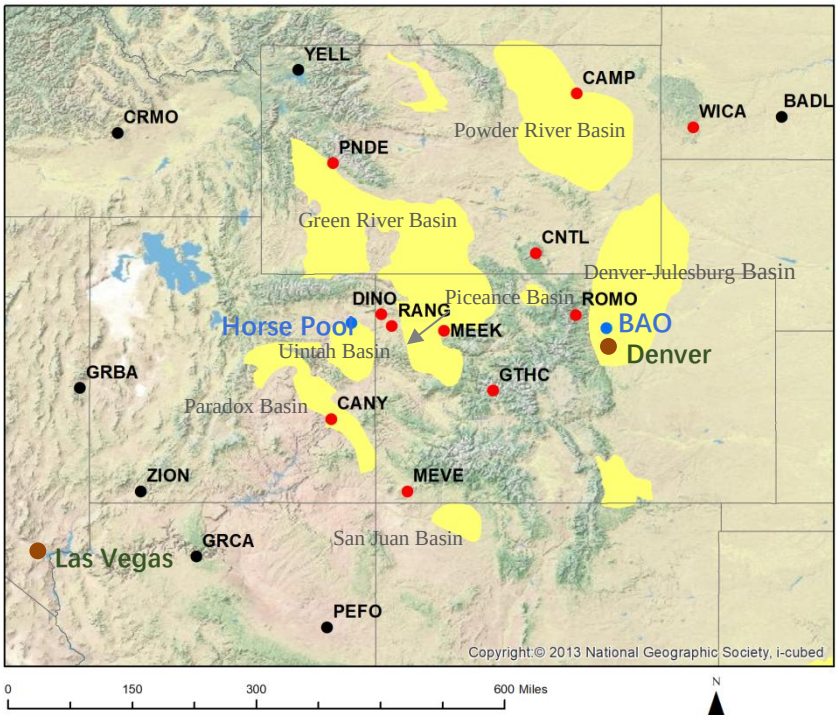

Figure 1. Topographic map of the mountain states with tight O&NG plays in the basins highlighted in yellow (https://www.eia.gov/). Eleven sites are located within 100km of a shale play (red dots), while seven sites are located at the periphery of the shale play (black dots). Blue dots show two campaign locations, Horse Pool and Boulder Atmospheric Observatory (BAO).

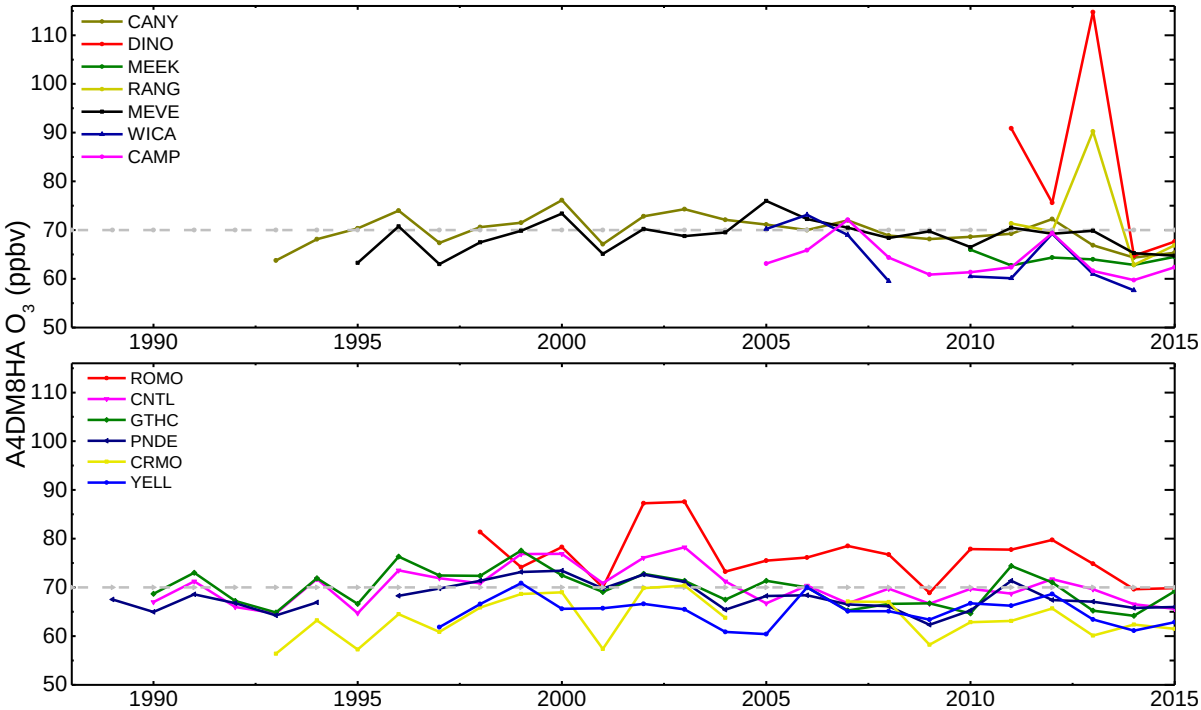

Figure 2. Time series of the A4DM8HA at each site. Dashed lines indicate the current ground-level O_3 standard (70 ppbv).

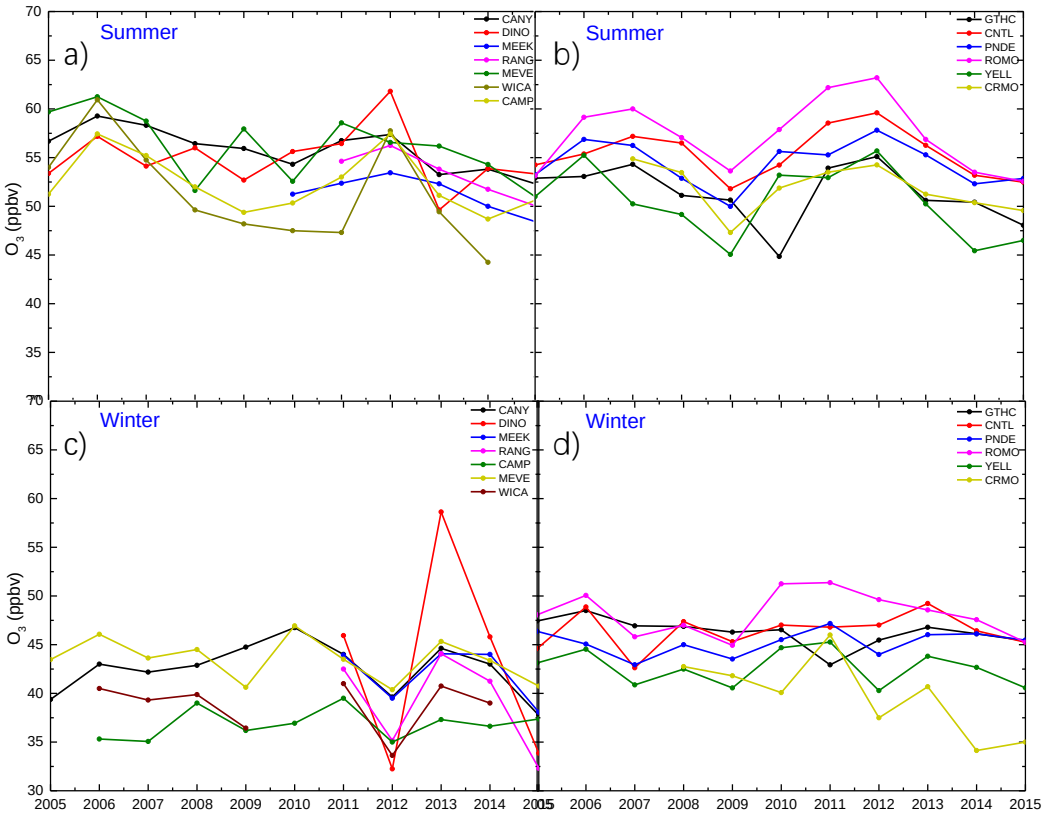

Figure 3. Time series of seasonal median values of DM8HA O_3 at each site in summer (a-b) and winter (c-d).

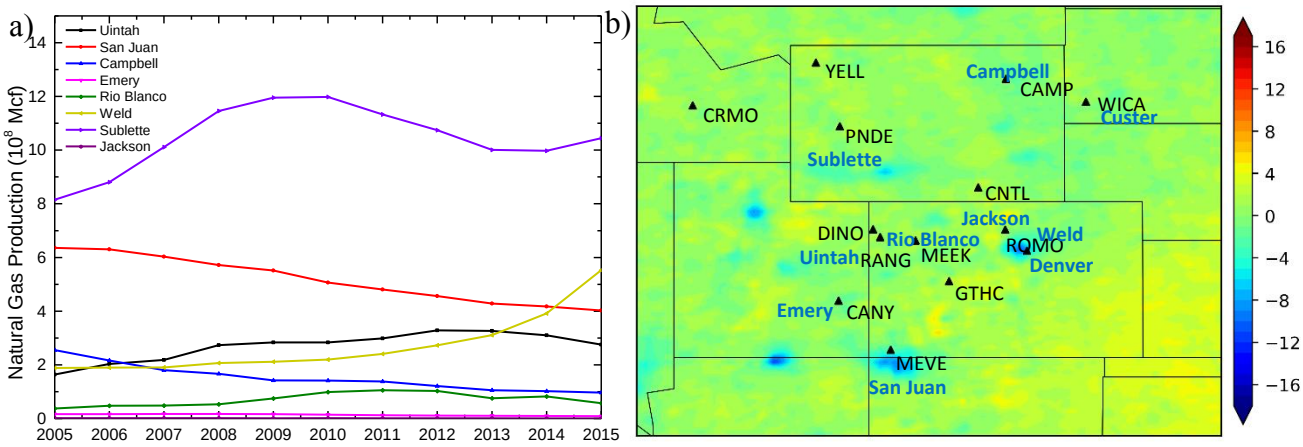

Figure 4. (a) Annual natural gas production in the counties that located in the O&NG basins over 2005 – 2015 (Data sources: the Utah Oil and Gas Program, https://oilgas.ogm.utah.gov/oilgasweb/index.xhtml; the Colorado Oil&Gas Conservation Commission, http://cogcc.state.co.us/data.html; the Wyoming Oil&Gas Conservation Commission, http://wogcc.wyo.gov/; the New Mexico Oil Conservation Division, http://www.emnrd.state.nm.us/ocd/). (b) The difference of OMI tropospheric NO_2 column densities (10^{14} molec.cm^{-2}) in summer between periods of 2005 – 2010 and 2011 – 2015. Yellow color indicates regions where NOx has increased between 2005 – 2010 and 2011 – 2015, while blue color indicates regions where NOx has decreased. (Data source: Tropospheric Emission Monitoring Internet Service (TEMIS), www.temis.nl).

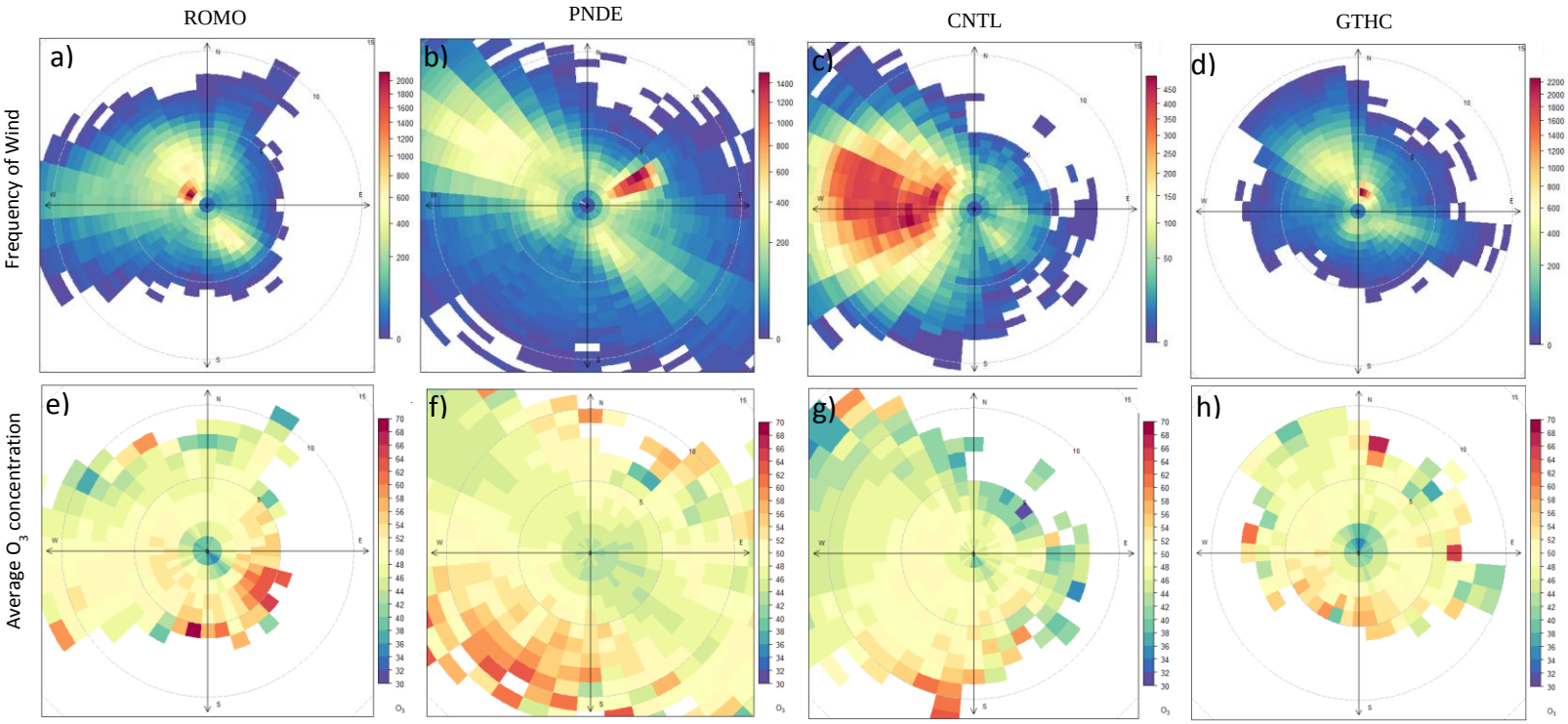

Figure 5. Frequency of wind (a-d) and average O_3 concentrations (ppbv) (e-h) binned by wind speed and wind direction at ROMO (a, e), PNDE (b, f), CNTL (c, g), and GTHC (d, h) over 2005 – 2015.

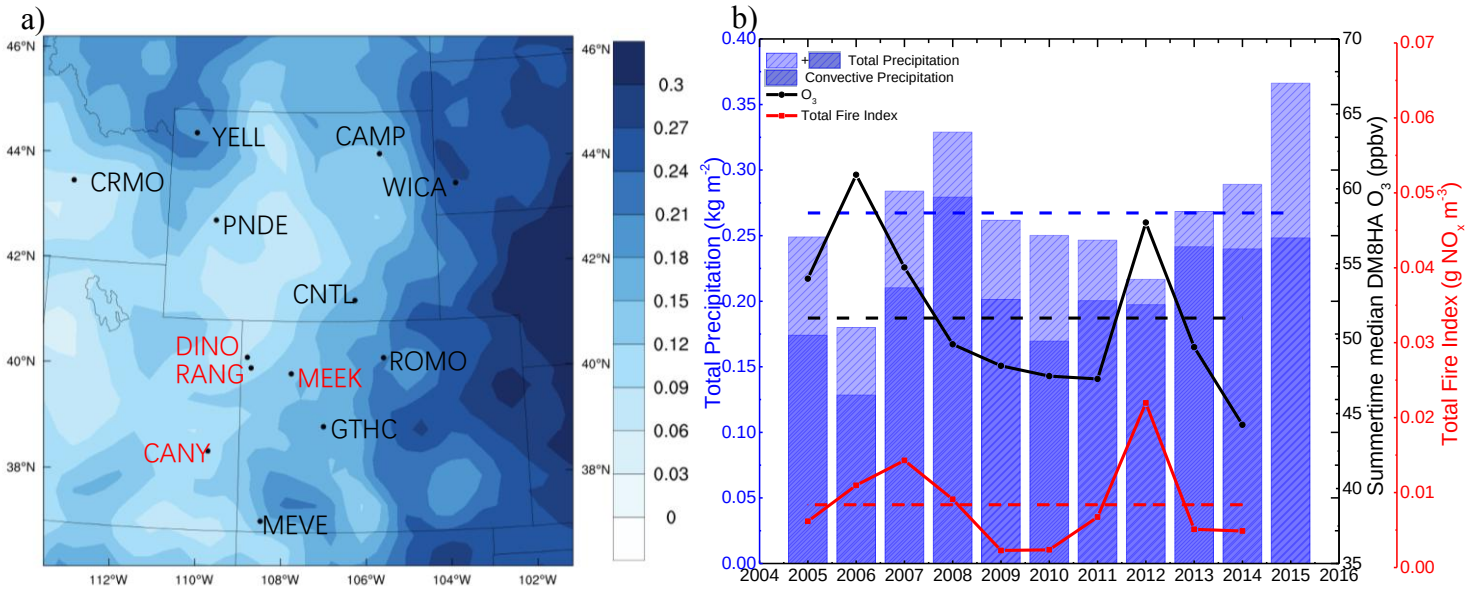

Figure ~~69~~. (a) Decadal average summertime total precipitation (kg m^{-2}) over 2005 – 2015, and the sites with low precipitation levels highlighted in red. (b) Time series of summer seasonal median DM8HA O_3, convective precipitation, total precipitation, and total fire index at WICA.

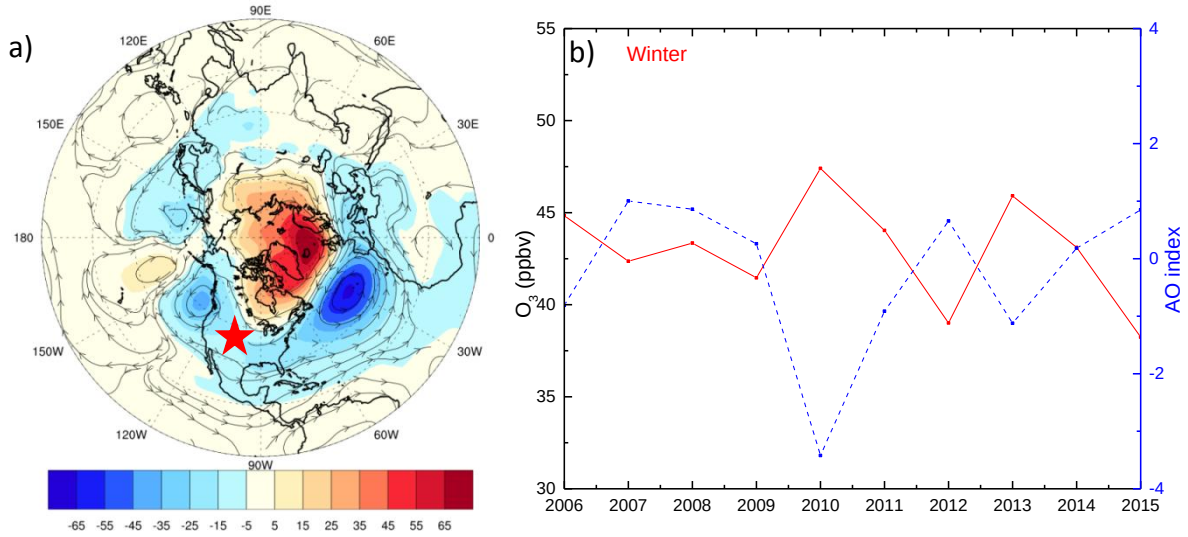

Figure 7~~6~~. (a) The difference of geopotential height (m) and streamlines at 850 hPa between the high (2006, 2008, 2010, 2011, 2013) and low O_3 years (2007, 2009, 2012, 2014, 2015). (b) Time series of median DM8HA O_3 averaged over the study region and the AO index in winter. The red star indicates the study region. (Source: NCEP/NCAR reanalysis)

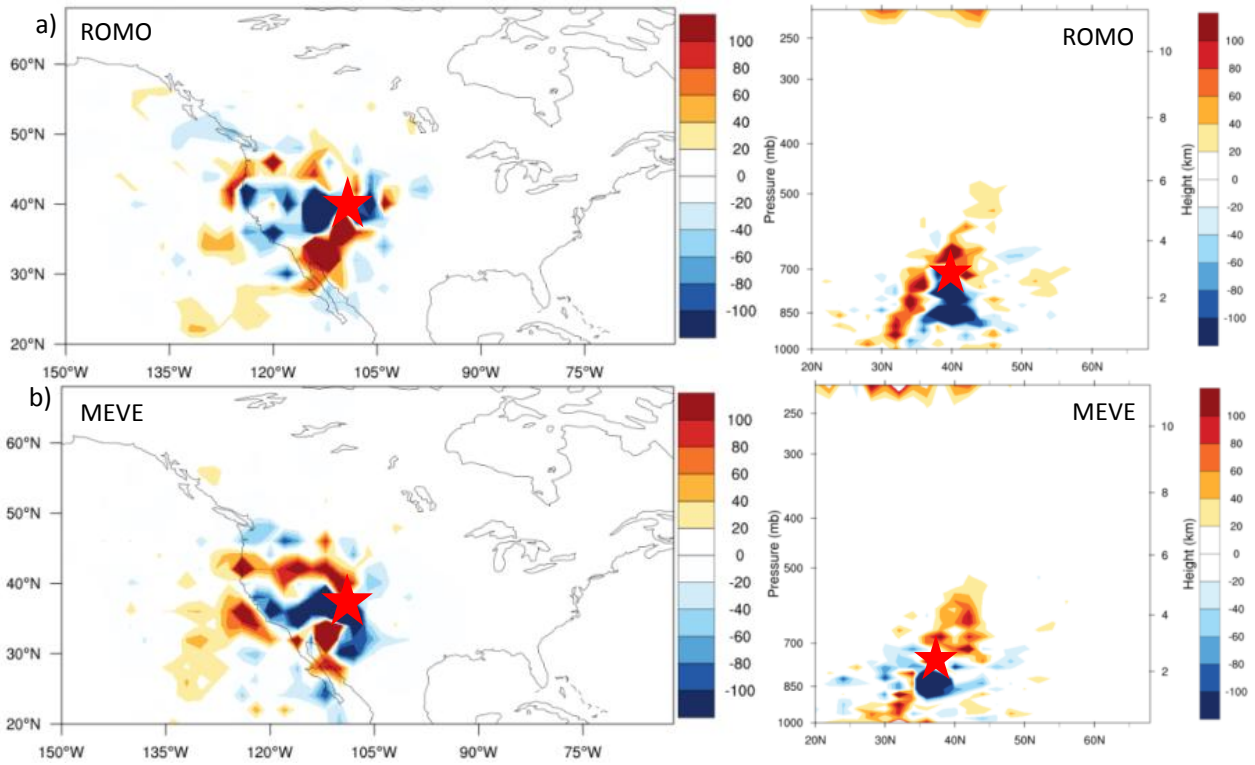

Figure 8~~7~~. Maps and cross sections of differences in the number of 5-day backward trajectories originating at (a) ROMO and (b) MEVE ~~(a) YELL, (b) MEVE, (c) WICA, (d) PNDE, (e) ROMO, and (f) CNTL~~ between high (2006, 2008, 2010, 2011, 2013) and low O_3 years (2007, 2009, 2012, 2014, 2015). Red stars indicate study sites. The red color indicates origins of air masses reaching the study site during high O_3 years, while blue color indicates locations of major air mass sources during low O_3 years.

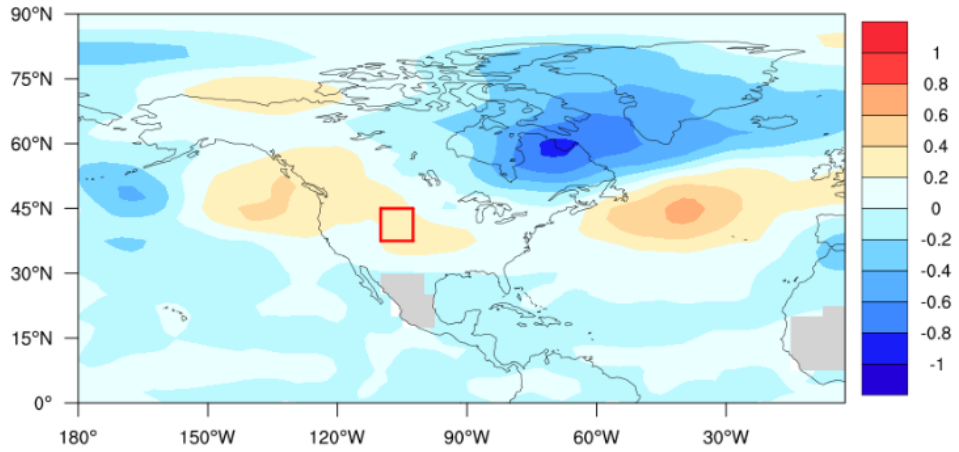

Figure 9~~8~~. The difference of potential vorticity (10^{-6} $m^2 s^{-1} kg^{-1} K$) at 315 K between the high O_3 years (2006,

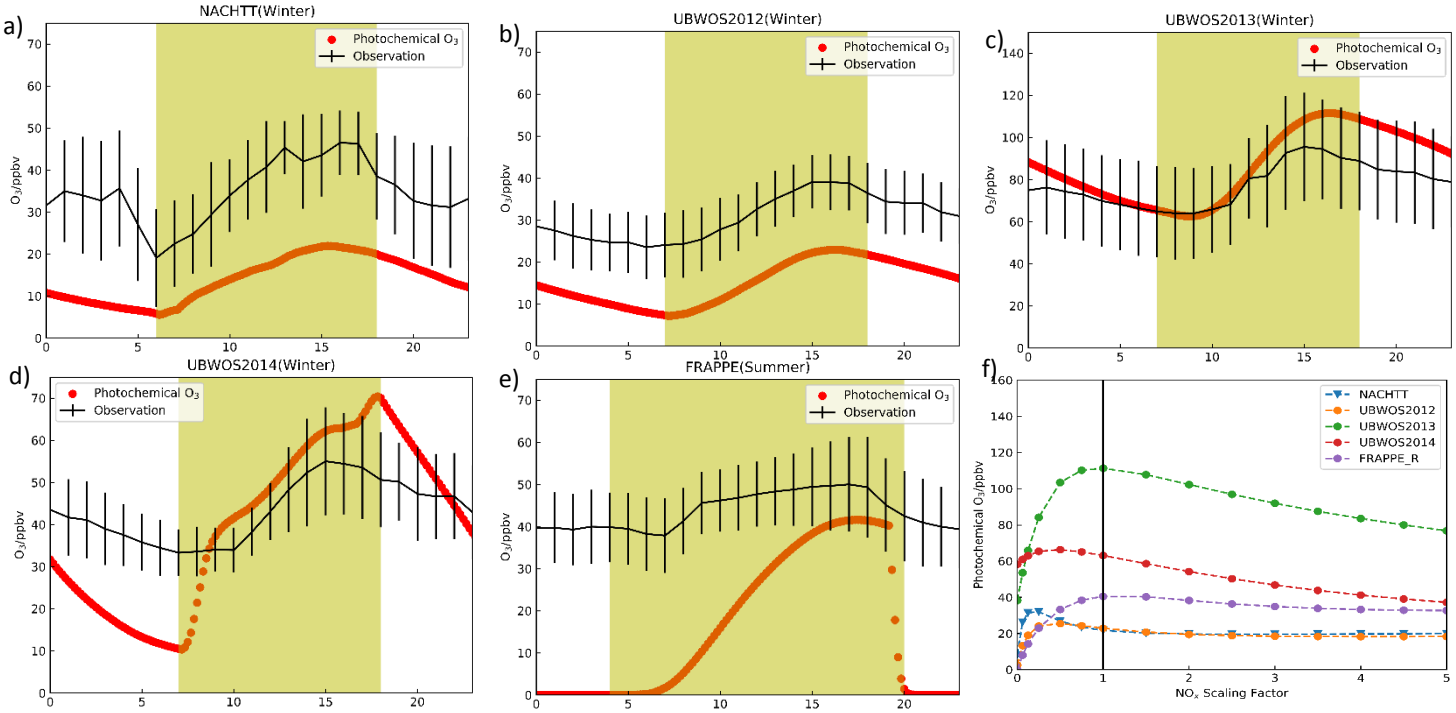

Figure 10. (a)-(e) Observed diel O_3 profile (black) and fully constrained base model calculated (red) for five campaigns. (f) NO_x sensitivity of maximum photochemical O_3 during each campaign. Shaded area indicated the time period between sunrise and sunset averaged over each campaign ~~The sensitivity of maximum photochemical O_3 to NO_x was tested by simulations with observed VOC concentrations and observed NO_x mixing ratios which was scaled by a factor from 0 to 5. NOx scaling factor of 1 indicated observed NOx mixing ratios.~~

Decadal Trends and Variability in Intermountain West Surface Ozone near Oil and Gas Extraction Fields

Ying Zhou[1], Huiting Mao[1], and Barkley C. Sive[2]

[1]Department of Chemistry, State University of New York College of Environmental Science and Forestry, Syracuse, NY, 13210, USA

[2]National Park Service, Air Resources Division, Lakewood, CO 80225, USA

Corresponding author: H. Mao (hmao@esf.edu)

Contents of this File

Text: Section S1 to S8

Figures: S1 to ~~S3~~S4

Tables: S1 to ~~S8~~S7

S1. ~~Locations of selected sites~~

~~Long-term ozone (O_3) observations were available at 18 rural sites in the U.S. Intermountain West and 11 sites were located within 100 km of the shale play (Figure 1 and Table S1). Data were obtained from the National Park Service (NPS), Clean Air Status and Trends Network (CASTNET), and Wyoming Department of Environmental Quality (WDEQ).~~

~~S2.~~ Identification of reference sites

~~The backward~~Backward trajectory cluster analysis was used to identify sites that were under the minimal influence of oil and natural gas (O&NG) ~~extractions~~extraction (Figure 1). ZION, GRCA, GRBA, and PEFO are located in the downwind area of Las Vegas (Figures S1c-f). Cluster analysis ~~indicated~~suggested that ~20% – 50% of air masses likely came from the direction of Las Vegas~~. In~~, NE, and in addition, ~30% of air masses at GRCA (Cluster 4) and PEFO (Cluster 3) passed Phoenix, AZ. Therefore, surface O_3 at ZION, GRCA, GRBA, and PEFO ~~could be~~was likely significantly influenced by ~~the nearby anthropogenic~~urban emissions. At BADL, Cluster 3 ~~indicated~~suggested that 32% of air masses was transported from the periphery of the Powder River Basin (Figure S1g). In comparison, nearly all clusters reaching YELL and CRMO were found be from the upwind areas of O&NG extraction. Therefore, YELL and CRMO were used as reference sites to investigate the decadal O_3 change.

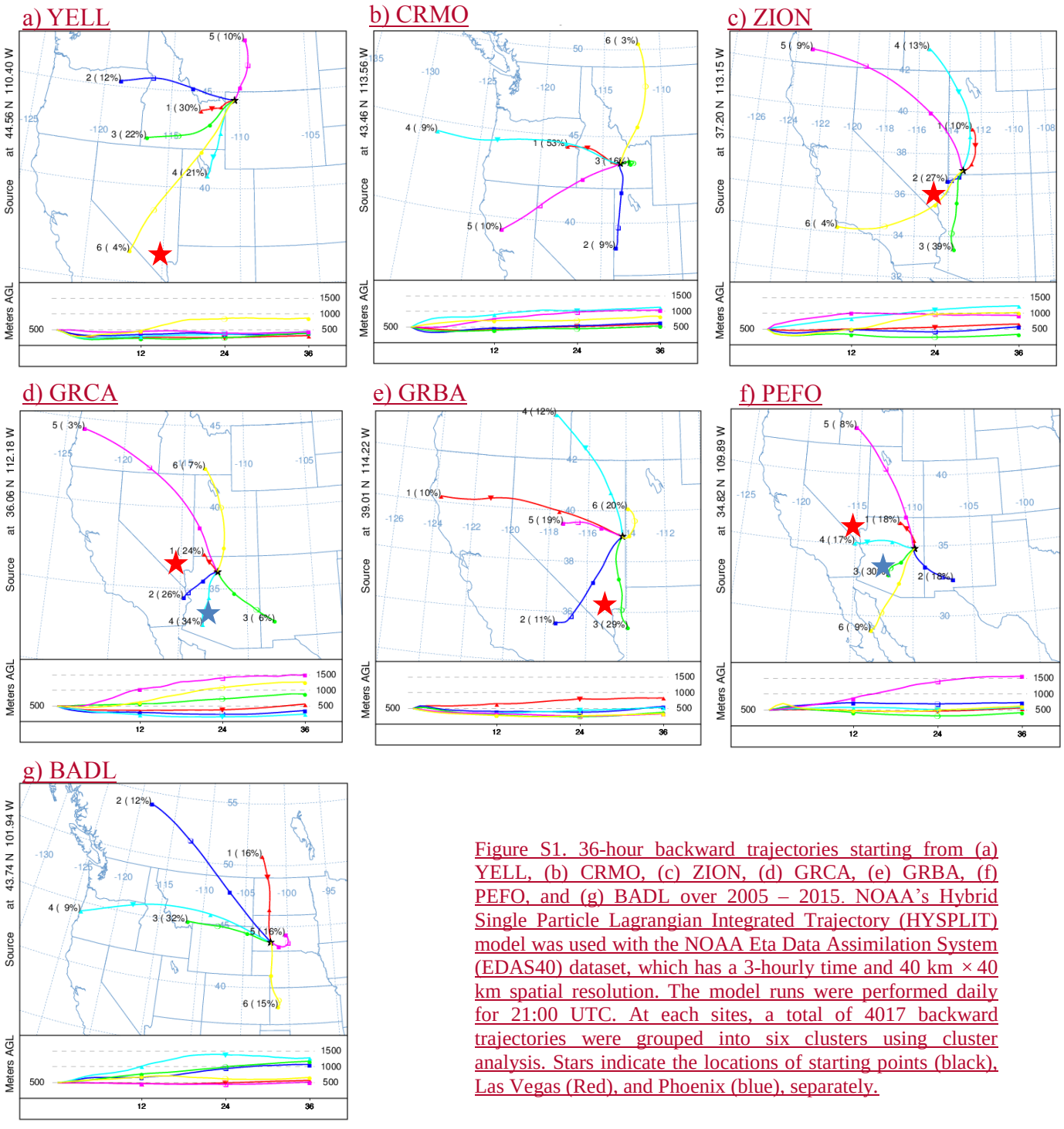

Figure S1. 36-hour backward trajectories starting from (a) YELL, (b) CRMO, (c) ZION, (d) GRCA, (e) GRBA, (f) PEFO, and (g) BADL over 2005 – 2015. NOAA's Hybrid Single Particle Lagrangian Integrated Trajectory (HYSPLIT) model was used with the NOAA Eta Data Assimilation System (EDAS40) dataset, which has a 3-hourly time and 40 km × 40 km spatial resolution. The model runs were performed daily for 21:00 UTC. At each sites, a total of 4017 backward trajectories were grouped into six clusters using cluster analysis. Stars indicate the locations of starting points (black), Las Vegas (Red), and Phoenix (blue), separately.

Table S1. Names and locations of sites used in this study.

Site Abbreviation	Park Unit/Measurement Network	Site	Latitude	Longitude	Elevation (m)	Start Date	End Date	Year-round Measurement
CANY	Canyonlands National Park	Island in the Sky	38.46	-109.82	1809	7/1/1992	12/30/2015	1993 - 2015
DINO	Dinosaur National Monument	West Entrance Housing	40.29	-108.94	1463	4/1/2005	12/30/2015	2011 - 2015
MEEK	Meeker	Plant Science	40.00	-107.85	1994	1/1/2010	12/30/2015	2010 - 2015
MEVE	Mesa Verde National Park	Resource Management Area	37.20	-108.49	2165	3/1/1993	12/30/2015	1995 - 2015
RANG	Rangely	Golf Course	40.09	-108.76	1655	8/1/2010	12/30/2015	2011 - 2015
ROMO	Rocky Mountain National Park	Long's Peak	40.28	-105.55	2743	4/1/1987	12/30/2015	1998 - 2015
WICA	Wind Cave National Park	Visitor Center	43.56	-103.48	1292	12/31/2003	12/30/2015	2005 - 2008; 2010 - 2014
CAMP	WDEQ	Campbell, WY	44.15	-105.53	1427	1/1/2005	12/31/2015	2005 - 2015
CNTL	CASTNET	Centennial, WY	41.36	-106.24	3175	5/9/1989	12/31/2015	1990 - 2015
GTHC	CASTNET	Gothic, CO	38.96	-106.99	2915	5/13/1989	12/31/2015	1990 - 2015
PNDE	CASTNET	Pinedale, WY	42.93	-109.79	2386	10/21/1988	12/31/2015	1989 - 1994; 1996 - 2015
BADL	Badlands National Park	Visitor Center	43.74	-101.94	739	10/1/1987	12/31/2014	1988 - 1991; 2004 - 2014
CRMO	Craters of the Moon National Monument & Preserve	Visitor Center	43.46	-113.56	1815	9/24/1992	12/30/2015	1993 - 2004; 2007 - 2015
GRBA	Great Basin National Park	Maintenance Yard	39.01	-114.22	2060	8/24/1993	12/30/2015	1994 - 2015
GRCA	Grand Canyon National Park	The Abyss	36.06	-112.18	2073	1/1/1993	12/30/2015	1993 - 2015
PEFO	Petrified Forest National Park	South Entrance	34.82	-109.89	1723	1/1/2002	12/30/2015	2003 - 2015
YELL	Yellowstone National Park	Water Tank	44.56	-110.40	2400	6/1/1996	12/30/2015	1997 - 2015
ZION	Zion National Park	Dalton's Wash	37.20	-113.15	1213	1/1/2004	12/30/2015	2004 - 2015

* MEEK and RANG are not located in national parks, but measurements at these two sites are also maintained by the NPS.

S2~~S3~~. Trends in surface ozone at each site

~~The~~US EPA's ozone design value (ODV) is defined as the 3 year running mean of the annual fourth-highest daily maximum 8 hour average (DM8HA) O_3 concentration. We calculated the annual fourth highest DM8HA (A4DM8HA) for the 13 monitoring sites and their trends were examined ~~through ordinary linear least square regression~~using Mann-Kendall before and after 2005. The trends were also calculated separately for 5th, 50th, 95th percentiles ~~of~~ DM8HA O_3 mixing ratios in summer and winter.

Table ~~S2~~S1. Trends in the A4DM8HA O_3 at each site before and after 2005. Boldfaced numbers indicate p-value≤0.10.

Site	Time Period	Trends	Time Period	Trends (ppbv yr^{-1})	Average (ppbv)
CANY	1993 - 2004	**0.~~55~~61 (0.06)**	2005 - 2015	**-0.~~54~~58 (0.~~02~~04)**	68.8
CAMP			2005 - 2015	-0.~~44~~38 (0.~~25~~24)	63.9
DINO			2011 - 2015		**82.7**
MEEK			2010 - 2015		64.1
RANG			2011 - 2015		**72.2**
MEVE	1995 - 2004	0.~~45~~53 (0.~~25~~47)	2005 - 2015	**-0.~~76~~83 (<0.01)**	69.4
ROMO	1998 - 2004	0.~~41~~29 (0.~~78~~99)	2005 - 2015	-0.~~46~~19 (0.~~23~~64)	**75.1**
WICA			2005 - 2014	**-1.~~21~~16 (0.~~05~~09)**	64.5
CTNL	1990 - 2004	**0.~~65 (<~~68 (0.~~01~~03)**	2005 - 2015	-0.~~06~~03 (0.~~78~~31)	68.4
GTHC	1990 - 2004	0.~~17~~10 (0.~~46~~62)	2005 - 2015	-0.~~16~~21 (0.~~64~~35)	68.1
PNDE	1989 - 2004	**042 (0.~~33 (0.03~~02)**	2005 - 2015	-0.~~08~~16 (0.~~75~~35)	66.8
CRMO	1993 - 2004	**0.~~79~~83 (0.~~06~~02)**	2007 - 2015	-0.~~50~~54 (0.~~23~~18)	63.1
YELL	1997 - 2004	-0.~~30~~18 (0.~~57~~54)	2005 - 2015	-0.~~17~~28 (0.58)	64.8

Table ~~S3~~S2. Trends in seasonal 5th, 50th, and 95th ~~percentiles of~~percentile DM8HA O_3 mixing ratios at each site in winter and summer over 2005 – 2015. Boldfaced numbers indicate p-value ≤0.10. Note that wintertime O_3 in a certain year referred to O_3 in January, February, and December in the previous year.

	Winter				Summer			
Site	Time Period	5th	50th	95th	Time Period	5th	50th	95th
CANY	2006 - 2015	-0.~~05~~19	-0.~~07~~33	-0.~~17~~45	2005 - 2015	**-0.53**	**-0.~~51~~50**	-0.~~40~~33
CAMP	2006 - 2015	0.~~17~~09	0.~~12~~17	-0.~~17~~16	2005 - 2015	-0.~~12~~06	-0.~~32~~28	-0.~~51~~42
DINO	-				2005 - 2015	-0.~~16~~21	-0.~~11~~15	-0.~~09~~01
MEVE	2006 - 2015	-0.~~41~~52	-0.~~22~~34	**-0.~~49~~67**	2005 - 2015	**-0.~~51~~47**	**-0.~~63~~60**	**-0.~~61~~69**
ROMO	2006 - 2015	0.~~22~~53	-0.~~04~~21	-0.~~21~~33	2005 - 2015	-0.~~13~~22	-0.~~13~~18	-0.~~34~~28
WICA	2006 - 2014	-0.~~23~~07	-0.~~16~~07	-0.~~30~~03	2005 - 2014	**-0.~~56~~1.60**	**-0.~~98~~1.02**	**-1.~~38~~60**
CTNL	2006 - 2015	0.~~15~~25	-0.13	-0.~~08~~35	2005 - 2015	-0.~~03~~06	-0.~~07~~12	0.~~14~~15
GTHC	2006 - 2015	-0.~~11~~04	**-0.~~24~~23**	**-0.~~36~~23**	2005 - 2015	-0.~~25~~18	-0.~~31~~35	-0.~~23~~25
PNDE	2006 - 2015	0.12	0.~~10~~17	-0.~~69~~27	2005 - 2015	0.~~26~~14	-0.~~07~~13	-0.~~10~~09
CRMO	2008 - 2015	-0.~~71~~76	**-1.~~18~~30**	**-1.~~10~~12**	2007 - 2015	-0.~~14~~16	-0.~~34~~54	-0.~~46~~57
YELL	2006 - 2015	-0.~~06~~04	-0.10	-0.~~55~~59	2005 - 2015	-0.~~25~~32	-0.~~39~~46	-0.~~11~~20

~~S4~~S3. Emissions in selected counties

Emissions of NOx and VOCs were obtained from EPA's National Emission ~~Inventory~~Inventories (NEI).

Table ~~S4~~S3. NO_x emissions in selected counties

			NOx emission (~~Ton~~ton)_O&NG Extraction				NOx emission (~~Ton~~ton)_total			
County	State	Basin	2005	2008	2011	2014	2005	2008	2011	2014
San Juan	New Mexico	San Juan Basin	263	351	14504	13906	80997	35626	44806	41902
Emery	Utah	Paradox Basin	0	0	88	158	30282	32814	22215	20729
Uintah	Utah	Uintah-Piceance Basin	0	0	10033	7412	8698	2049	11897	9407
Campbell	Wyoming	Powder River Basin	0.33	2407	505	2301	12142	22195	44429	18702
Sublette	Wyoming	Greater Green River Basin	0	5977	2501	4188	2369	9091	4970	5792
Jackson	Colorado	North Park Basin	0	0	2	107	243	442	632	573
Rio Blanco	Colorado	Uintah-Piceance Basin	7	190	1434	4021	2020	3914	5027	6997
Weld	Colorado	Denver-Julesburg Basin	0	76	12478	17892	13112	20088	32696	33275
Custer	South Dakota		0	0	2.25	0.45	1156	1309	1727	1373

Table ~~S5~~S4. VOC emissions in selected counties

			VOC emission (~~Ton~~ton)_O&NG Extraction				VOC emission (~~Ton~~ton)_total			
County	State	Basin	2005	2008	2011	2014	2005	2008	2011	2014
San Juan	New Mexico	San Juan Basin	142	512	22089	32819	8858	58095	88840	97096
Emery	Utah	Paradox Basin	0	0	459	549	1715	43441	46945	37107
Uintah	Utah	Uintah-Piceance Basin	0	0	76502	86915	4545	40044	116207	126578
Campbell	Wyoming	Powder River Basin	52	2697	6703	8559	9558	35514	48870	34363
Sublette	Wyoming	Greater Green River Basin	5	15863	9079	58304	1558	70276	45282	86146
Jackson	Colorado	North Park Basin	28	57	516	688	1125	17402	20813	12850
Rio Blanco	Colorado	Uintah-Piceance Basin	0.4	1092	23432	6141	1647	34518	57809	38601
Weld	Colorado	Denver-Julesburg Basin	0	713	104473	91709	12846	52991	150982	116146
Custer	South Dakota		0	0	12	1	1789	27132	29169	19210

S5. Wintertime O_3 at Edmonton, Alberta, Canada

Ozonesonde data at Edmonton were obtained from the World Ozone and Ultraviolet Radiation Data Center (http://woudc.org/data/products/ozonesonde/). Significant negative correlation (r = -0.49, p = 0.01) was found between lower tropospheric O_3 at Edmonton and the AO index over the winter of 1988 – 2014 (Figure S2).

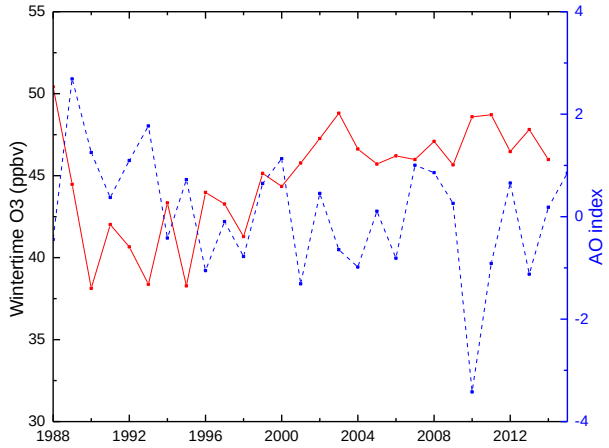

Figure S2.Time series of lower tropospheric (2 – 5 km) O_3 at Edmonton (53.55 °N, 114.10 °W) and the AO index in winter.

S6S4. Fire index

TheNOAA's Lagrangian dispersion model, Hybrid Single-Particle Lagrangian Integrated Trajectory (HYSPLIT) model, was used to estimate O_3 concentrations determined by wildfire emissions. HYSPLIT simulated the long-range and mesoscale transport, diffusion, and dry and wet deposition of gas or particles (Draxler & Hess, 1998). The National Center for Environmental Prediction (NCEP) Eta Data Assimilation System (EDAS40) datasets, with a 3-hourly time and 40 km × 40 km spatial resolution, were used to drive the Lagrangian dispersion model. For each day over summer 2005 – 2015, 250,000 particles were released at a constant hourly rate during the first 24 h at a height of 100 m overat each measurement site. A decay half-life of five days occurred to the particle mass (Lu et al., 2016) and the particles were traced

backward for five days. The retroplumes of each sample were calculated daily in 0.25 ° × 0.25 ° horizontal resolution from the surface to 5 km. In total, we have computed over 4950 HYSPLIT retroplumes for each Intermountain West site.

The Global Fire Emissions Database version 4.1 (GFED4s) ~~were~~was used to provide information ~~of~~on biomass burning emissions. GFED4s ~~had~~has a spatial resolution of 0.25 ° × 0.25 °and ~~contained~~contains monthly burned area, fire carbon and dry matter emissions (DM), as well as daily fraction and contributions of different fire types to the total emissions since 2003. The fire types ~~included~~include savanna, grassland, and shrubland fires, boreal forest fires, temperature forest fires, tropical deforestation and degradation fires, peatland fires, and agricultural waste burning. Biomass burning ~~was complex and the~~ emissions ~~depended~~depend greatly on the ecosystem type (Jaffe et al., 2008). Akagi et al. (2011) found that wildfire emissions had a relatively high VOC/NO_x ratio of ~10 – 100 and O_3 production in smoke plumes was very sensitive to NO_x concentrations. Different from previous studies (Jaffe et al., 2008; Lu et al., 2016) using monthly or daily wildfire burned areas, we estimated daily wildfire NO_x emissions using monthly DM emissions, daily fraction, and fractional contribution of fire types in combination of emission factors (Akagi et al. 2011). Based on Lu et al. (2016), we then calculated a fire index (FI) as the product of daily HYSPLIT residence time and daily wildfire NO_x emission, in units of g NO_x m^{-3}. The sum of FI over the 5-day period was defined as total fire index (TFI):

$$FI(n) = \sum_i \sum_j \sum_k E_{DM}(i,j) \times t_r(i,j,n) \times F_{daily}(i,j,n) \times F_{type}(k)$$

$$TFI = \sum_{n=1}^{5} FI(n)$$

where $E_{DM}(i, j)$ was the monthly wildfire dry matter emission in the model grid cell i (longitude) and j (latitude), $F_{daily}(i, j, n)$ was the daily fraction of wildfire emissions, $F_{type}(k)$ was the NO_x

emission factor from fire type *k*, $t_{r(i, j, n)}$ was HYSPLIT calculated daily residence time, and *n* defined the backward day in the 5-day period. The summertime wildfire NO_x impacts were computed by averaging the daily TFI index.

~~S7~~S5. Impacts of wildfire emissions on summertime O_3

In contrast to wintertime O_3 levels, summertime median DM8HA O_3 displayed significant interannual variations with large differences between sites (Figure 3). The TFI, calculated with HYSPLIT dispersion model simulations and wildfire NO_x emissions, ~~varied~~showed large interannual variation at each site over 2005 – 2015 (Figure ~~S3~~S2). In 2012, the western U.S. experienced widespread drought with hot weather causing frequent wildfires across the region (Abeleira & Farmer, 2017). The decadal highest TFI value (0.013 – 0.052 g NO_x m^{-3}) in summer 2012 were observed at CRMO and YELL, as well as 9 other sites (DINO, MEEK, RANG, ROMO, WICA, CAMP, CNTL, PNDE, and GTHC) (Figure ~~S3~~S2), which was mostly consistent with the observed decadal highest summertime median DM8HA O_3 at the same sites except WICA (54 – 65 ppbv).

Significant positive correlations between summertime O_3 and TFI were found at the reference site YELL, as well as at CANY, CAMP, DINO, MEVE, WICA, CNTL, GTHC, and PNDE during their respective time periods over 2005 – 2015 (Table ~~2~~S5). It should be noted that significant ~~correlation was~~ correlations were found for seasonal 75th or 95th ~~percentiles~~ percentile DM8HA O_3 mixing ratios with TFI at YELL, CANY, GTHC, PNDE, and MEVE. Strong correlations, albeit not statistically significant, were also found between TFI and summertime 95th percentile DM8HA O_3 at RANG (Table ~~S6~~S5). As indicated by data at the reference site YELL, the wildfire emissions had a larger impact on high O_3 levels in summer over the Intermountain West. While wintertime O_3 at CANY, DINO, and RANG was strongly impacted

by photochemical production from O&NG emissions within the basins (Section ~~5~~6), during the summer, the interannual variability of O_3 at 8 out of 11 sites near the O&NG extraction fields appeared to be predominantly impacted by photochemical production from wildfire emissions.

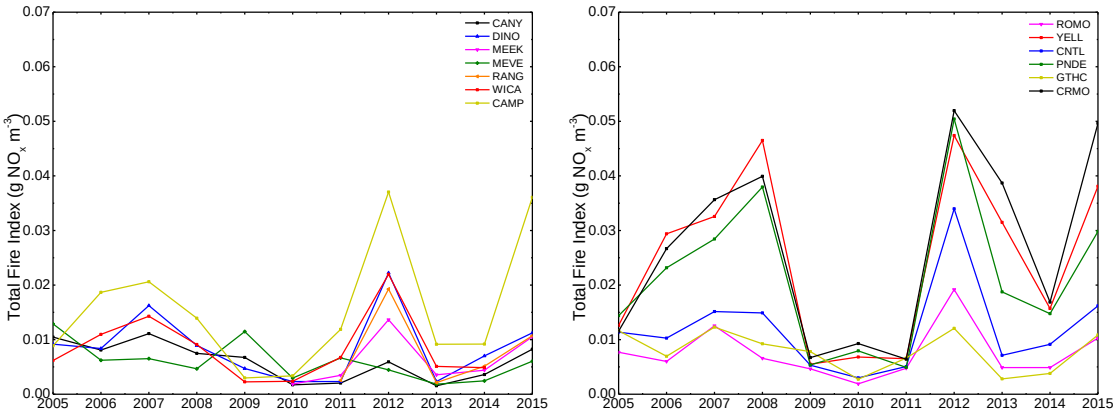

Figure ~~S3~~S2. Time series of summertime total fire index at each site.

Table ~~S6~~S5. Correlation ~~coefficient~~coefficients (r) and p-~~value~~values in parenthesis between the pairs of variables over the summer of 2005 – 2015. Boldfaced numbers indicate p-value ≤0.10.

		r(O_3 vs TFI)			Partial r	Regression	r(O_3 vs Relative Humidity)			Partial r
Site	Time Period	5th	50th	95th	95th	Intercept_50th	5th	50th	95th	5th
CANY	2005 - 2015	0.20 (0.55)	0.47 (0.14)	0.37 (0.26)	0.32 (0.40)	**54.01**	**-0.65 (0.08)**	-0.50 (0.11)	-0.01 (0.97)	**-0.61 (0.07)**
CAMP	2005 - 2015	0.33 (0.33)	**0.57 (0.06)**	0.50 (0.12)	0.22 (0.57)	**50.08**	-0.45 (0.19)	**-0.92 (<0.01)**	**-0.66 (0.04)**	**-0.88 (<0.01)**
DINO	2005 - 2015	**0.62 (0.04)**	**0.58 (0.06)**	**0.62 (0.04)**	**0.67 (0.10)**	**52.42**	-0.14 (0.72)	-0.18 (0.64)	-0.21 (0.59)	**0.74 (0.06)**
MEEK	2010 - 2015	0.13 (0.81)	0.01 (0.99)	0.45 (0.37)	0.35 (0.56)	**51.28**	**-0.77 (0.06)**	-0.71 (0.11)	-0.31 (0.55)	**-0.85 (0.07)**
RANG	2011 - 2015	0.34 (0.57)	0.26 (0.67)	0.76 (0.24)	0.07 (0.92)	**52.58**	**-0.90 (0.03)**	-0.62 (0.26)	-0.32 (0.60)	**-0.91 (0.09)**
MEVE	2005 - 2015	0.39 (0.24)	0.50 (0.11)	**0.66 (0.03)**	0.42 (0.26)	**53.21**	-0.49 (0.12)	-0.46 (0.14)	-0.36 (0.28)	-0.43(0.25)
ROMO	2005 - 2015	0.28 (0.39)	0.40 (0.22)	0.40 (0.21)	0.53 (0.12)	**54.89**	-0.40 (0.22)	**-0.67 (0.02)**	**-0.80 (<0.01)**	**-0.58 (0.09)**
WICA	2005 - 2014	**0.65 (0.04)**	**0.71 (0.02)**	**0.57 (0.08)**	-0.42 (0.30)	**46.18**	**-0.71 (0.02)**	**-0.97 (<0.01)**	**-0.90 (<0.01)**	**-0.79 (0.02)**
CNTL	2005 - 2015	**0.59 (0.06)**	0.49 (0.12)	0.36 (0.28)	-0.13 (0.83)	**53.69**	-0.69 (0.13)	**-0.74 (0.09)**	-0.38 (0.45)	-0.44 (0.46)
GTHC	2005 -2015	0.28 (0.40)	**0.55 (0.08)**	**0.49 (0.03)**	**0.67 (0.09)**	**47.76**	0.24 (0.65)	-0.19 (0.72)	-0.21 (0.69)	0.45 (0.45)
PNDE	2005 - 2015	0.46 (0.16)	0.41 (0.21)	**0.53 (0.09)**	-0.06 (0.89)	**52.96**	**-0.58 (0.10)**	-0.67 (0.55)	**-0.78 (0.01)**	**-0.70 (0.05)**
CRMO	2007 -2015	-0.45 (0.22)	0.33 (0.38)	0.29 (0.44)	-0.26 (0.58)	**50.58**	0.36 (0.48)	**-0.89 (0.02)**	**-0.91 (0.01)**	**-0.87 (0.05)**
YELL	2005 - 2014	0.01 (0.49)	0.14 (0.34)	**0.50 (0.05)**	-0.03 (0.95)	**49.57**	**-0.56 (0.04)**	**-0.70 (0.01)**	**-0.81 (<0.01)**	**-0.70 (0.03)**

Regression equations were used to quantify the relationship between seasonal median DM8HA O_3 and TFI, where the intercepts from the equations represented decadal summertime median DM8HA O_3 values in the absence of fires (Jaffe et al., 2008). No significant positive correlation was found between summertime O_3 and TFI at ROMO, and ~~TFI, while~~ the O_3

concentration without wildfires (55 ppbv), based on the intercept value, was found to be the highest at this site. As stated in Section 4, ROMO was influenced by the high O_3 concentrations from the southeast over 2005 – 2015 (Figure 5). Summertime O_3 at ROMO was under strong influence of frequent transport of highly polluted air masses ~~emerging~~ from the greater Denver area, which likely dominated over the impact of wildfire emissions during the decade of the study period. Reddy and Pfister (2016) also found significant correlations between July DM8HA O_3 and 500hPa heights, particularly in areas of elevated terrain near urban sources of O_3 precursors.

S6. Wintertime O_3 at Edmonton, Alberta, Canada

Ozonesonde data at Edmonton were obtained from the World Ozone and Ultraviolet Radiation Data Center (http://woudc.org/data/products/ozonesonde/). Significant negative correlation (r = -0.49, p = 0.01) was found between lower tropospheric O_3 at Edmonton and the AO index over the winter of 1988 – 2014 (Figure S3).

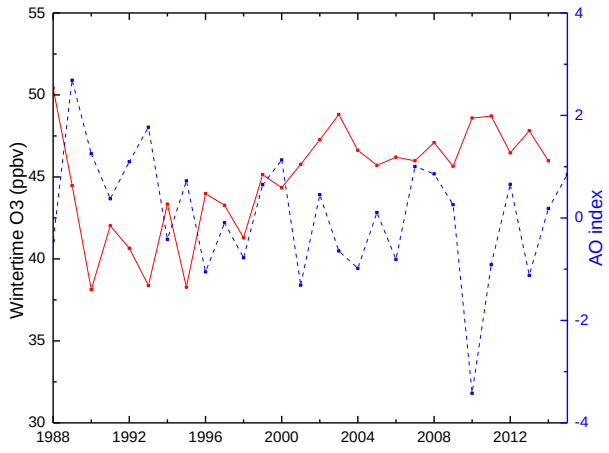

Figure S3.Time series of lower tropospheric (2 – 5 km) O_3 at Edmonton (53.55 ℃N, 114.10 ℃W) and the AO index in winter.

S7. Contributions of transport from the Arctic and West Coast

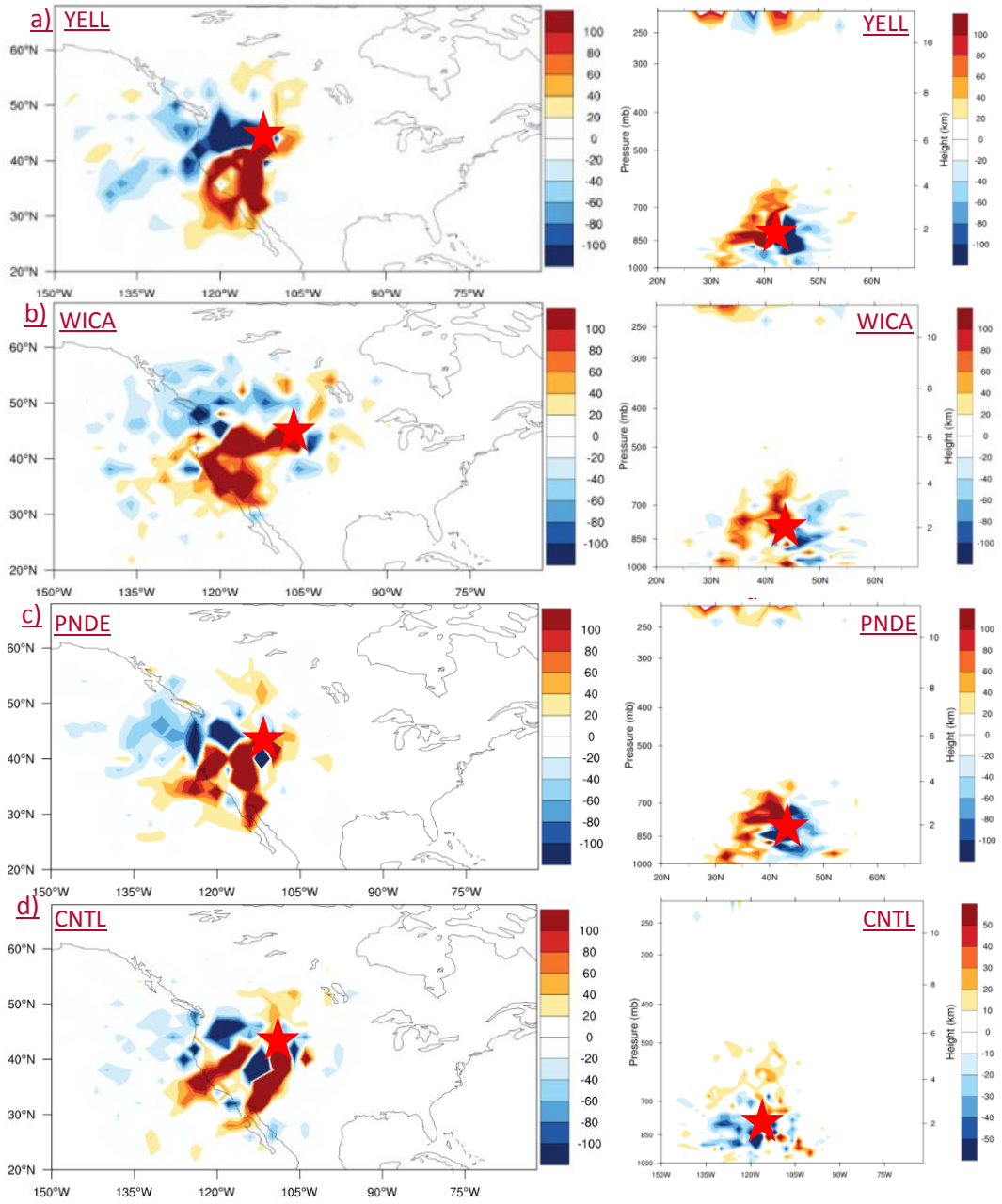

Figure S4. Maps and cross sections of differences in the number of 5-day backward trajectories originating at (a) YELL, (b) WICA, (c) PNDE, (d) CNTL, and between high (2006, 2008, 2010, 2011, 2013) and low O_3 years (2007, 2009, 2012, 2014, 2015). Red stars indicate study sites. Red color indicates regions and heights from where more air masses reached the study site in high O3 years, while blue color indicates locations of air mass sources in low O3 years.

S8. BOXMOX Model Simulations

S8.1 Field Campaigns

Surface observations were obtained from five field campaigns to constrain model simulations (Tables ~~S7–8~~S6–7). The Nitrogen, Aerosol Composition, and Halogens on a Tall Tower (NACHTT) campaign was conducted at the National Oceanic and Atmospheric Administration's Boulder Atmospheric Observatory (BAO). BAO is located in a primarily agricultural region and is very close to major urban areas. It is ~35 km north of Denver and ~30 km east of Boulder. In addition, the site is located within the Denver-Julesburg Basin, which is an active ~~oil and gas~~O&NG exploration and production region. The Uintah Basin Winter Ozone Studies (UBWOS) were a set of field campaigns held at Horse Pool during January and February of 2012, 2013, and 2014. Horse Pool is a remote site, located within the oil and gas basin of northeastern Utah. In summer 2014, the NSF Front Range Air Pollution and Photochemistry Experiment (FRAPPÉ) and the NASA Deriving Information on Surface Conditions from Column and Vertically Resolved Observations Relevant to Air Quality (DISCOVER-AQ) field campaigns conducted aircraft, mobile, and ground-based measurements over 15 locations across the Front Range. In this study, we used field measurements at ROMO-LP. All campaign data were available at https://esrl.noaa.gov/csd /groups/csd7/measurements/.

Table ~~S7. Name~~S6. Names and locations of campaign sites used in this study

Campaign	Time Period	State	Site	Elevation/km	Latitude	Longitude
NACHTT	02182011-03132011	Colorado	BAO	1.58	40.05	-105.01
UBWOS2012	01172012-02222012	Utah	Horse Pool	1.53	40.14	-109.47
UBWOS2013	02012013-02212013	Utah	Horse Pool	1.53	40.14	-109.47
UBWOS2014	01182014-02142014	Utah	Horse Pool	1.53	40.14	-109.47
FRAPPÉ	07172014-09032014	Colorado	ROMO-LP	2.74	40.28	-105.55

S8.2 Photolysis Rates

The model used the NCAR TUV radiation model to calculate photolysis frequencies, with inputs for latitude, longitude, altitude, Julian day, temperature, surface pressure, total O_3 column, and albedo. Inputs of surface temperature and pressure were constrained to measurements from field campaigns, while total O_3 column was derived from averaged OMI data. The TUV calculated photolysis frequencies were then scaled to the observed $j(NO_2)$, except for $j(O^1D)$. Measurement of $j(NO_2)$ was not available for UBWOS2013, UBWOS2014, and FRAPPÉ. Instead, total downwelling radiation measurements from these three campaigns were used to calculate photolysis frequencies by comparison with data from UBWOS2012 (Edwards et al. 2014). Polynomial regression was used to find the relationship between downwelling solar radiation versus $j(NO_2)$ using data from UBWOS2012 (E1). Then, $j(NO_2)$ during UBWOS2013, UBWOS2014, and FRAPPÉ was calculated using the derived equation (E1).

~~$j(NO_2) = 5.509\times10^{-6} + 1.425\times10^{-5} \times Radiation_{downwelling} - 4.760\times10^{-9} \times Radiation_{downwelling}^2$~~ ~~E1~~

$j(NO_2) = 1.425\times10^{5}\ Radiation_{downwelling} + 4.760\times10^{9}\ Radiation_{downwelling}^2$ (E1)

S8.3 Turbulent Mixing

Mixing ratios of CO, CH_4, NO, NO_2, and non-methane VOCs were constrained to observations by introducing turbulent mixing. This was represented by adding the background concentration of a species outside the box (Knote et al., 2015).

$$\frac{\partial c_{box}}{\partial t} = \frac{1}{\tau}(c_{bg} - c_{box}(t = t_0))$$

$$c_{box}(t = t_0 + \Delta t) = c_{box}(t = t_0) + \frac{\partial c_{box}}{\partial t} \cdot \Delta t$$

Where t_0 was the beginning of the time step, τ the mixing time-scale, c_{bg} the background concentrations of a species i outside the box, and c_{box} the initial concentration of the species i.

S8.4 Physical loss

First order rate constants were used to simulate all non-chemical loss in the model due to surface deposition. ~~Dry~~A dry deposition ~~rates~~velocity of 0.4 cm/s ~~were~~was used for O_3 over the continent and 0.07 cm/s over the snow~~,~~ based on Hauglustaine et al. (1994).

~~TableS8~~TableS7. Chemical observations used to inform the box model analysis in this analysis.

	Observational technique				
Compound	NACHTT	UBWOS2012	UBWOS2013	UBWOS2014	FRAPPÉ
O_3	CRDS	CRDS	CRDS	CRDS	
H_2O					
NO	CRDS	CRDS	CRDS	CRDS	No_noxbox
NO_2	CRDS	CRDS	CRDS	CRDS	NO2_Noxbox
N2O5	CRDS	CRDS	CRDS	CRDS	
HNO_3	CIMS	CIMS	CIMS	HR-TOF-CIMS	
HONO	CIMS	CIMS	CIMS	HR-TOF-CIMS	
CO	Thermo 48C	VUF	VUF	VUF	
Alkanes					
Methane	1.8 ppmv	CRDS	CRDS	CRDS	1.8 ppmv
Ethane	GC-MS*	GC-MS	GC-FID	GC-MS	GC-MS*
Propane	GC-MS*	GC-MS	GC-FID	GC-MS	GC-MS*
n-Butane	GC-MS*	GC-MS	GC-FID	GC-MS	GC-MS*
iso-Butane	GC-MS*	GC-MS	GC-FID	GC-MS	GC-MS*
n-Pentane	GC-MS*	GC-MS	GC-FID	GC-MS	GC-MS*
iso-Pentane	GC-MS*	GC-MS	GC-FID	GC-MS	GC-MS*
n-Hexane	GC-MS*	GC-MS	GC-FID	GC-MS	GC-MS*
n-Heptane	GC-MS*	GC-MS	GC-FID	GC-MS	GC-MS*
n-Octane	GC-MS*	GC-MS		GC-MS	GC-MS*
n-Nonane	GC-MS*	GC-MS		GC-MS	GC-MS*
n-Decane	GC-MS*	GC-MS		GC-MS	
Undecane	GC-MS	GC-MS			
2-Methylpentane	GC-MS*	GC-MS	GC-FID	GC-MS	
3-Methylpentane	GC-MS*	GC-MS	GC-FID	GC-MS	
2,2-Dimethylbutane	GC-MS*	GC-MS	GC-FID	GC-MS	
2,3-Dimethylbutane	GC-MS*				
2-Methylhexane	GC-MS*				

3-Methylhexane				GC-MS	
Cyclohexane	GC-MS*	GC-MS	PTR-MS[1]	GC-MS	
Neopentane	GC-MS*	GC-MS	GC-FID		
Aromatics					
Benzene	GC-MS*	GC-MS	GC-FID	GC-MS	GC-MS*
Toluene	GC-MS*	GC-MS	PTR-MS	GC-MS	GC-MS*
Ethyl Benzene	GC-MS*	GC-MS	PTR-MS[1]	GC-MS	GC-MS*
n-Propyl Benzene	GC-MS*	GC-MS	PTR-MS[1]	GC-MS	
iso-Propyl Benzene	GC-MS*	GC-MS	PTR-MS[1]	GC-MS	
m-Xylene	GC-MS*	GC-MS	PTR-MS[1]	GC-MS	GC-MS*
p-Xylene	GC-MS*	GC-MS		GC-MS	GC-MS*
o-Xylene	GC-MS*	GC-MS	PTR-MS[1]	GC-MS	GC-MS*
1,3,5-Trimethylbenzene	GC-MS*	GC-MS	PTR-MS[1]	GC-MS	
1,2,3-Trimethylbenzene	GC-MS*	GC-MS	PTR-MS[1]	GC-MS	
1,2,4-Trimethylbenzene	GC-MS*	GC-MS	PTR-MS[1]	GC-MS	
m-Ethyltoluene	GC-MS*			GC-MS	
p-Ethyltoluene	GC-MS*			GC-MS	
o-Ethyltoluene	GC-MS*	GC-MS	PTR-MS[1]	GC-MS	
Styrene	GC-MS*	GC-MS			
Alkenes and Alkynes					
Ethyne (Acetylene)	GC-MS*	GC-MS	GC-FID	GC-MS	GC-MS*
Ethene	GC-MS*	GC-MS	GC-FID	GC-MS	GC-MS*
Propene	GC-MS*	GC-MS	GC-FID	GC-MS	GC-MS*
1-Butene	GC-MS*				GC-MS*
trans-2-Butene	GC-MS*				GC-MS*
cis-2-Butene	GC-MS*				GC-MS*
iso-Butene					GC-MS*
1-Pentene	GC-MS*				
trans-2-Pentene	GC-MS*				
cis-2-Pentene	GC-MS*				
2-Methyl-1-Butene	GC-MS*				
2-Methyl-2-Butene	GC-MS*				
1,3-Butadiene		GC-MS			
Aldehydes and Ketones					
Acetone	GC-MS	GC-MS	PTR-TOF-MS	GC-MS	PTR-MS
2-Butanone (Methyl Ethyl Ketone)	GC-MS	GC-MS	PTR-TOF-MS	GC-MS	PTR-MS
Formaldehyde	PTR-MS	PTR-MS	PTR-MS	PTR-TOF-MS	
Acetaldehyde	GC-MS	GC-MS	PTR-TOF-MS	GC-MS	PTR-MS
Propanal	GC-MS	GC-MS		GC-MS	
Butanal		GC-MS		GC-MS	

Hexanal		GC-MS		GC-MS	
2-Propenal (Acrolein)					
Benzaldehyde		GC-MS			
Alcohols					
Methanol	GC-MS	GC-MS	PTR-TOF-MS	GC-MS	PTR-MS
Ethanol	GC-MS	GC-MS			
iso-Propanol	GC-MS				
1-Butanol	GC-MS				
Biogenics					
Isoprene	GC-MS	GC-MS			GC-MS*
Methyl Vinyl Ketone	GC-MS	GC-MS	PTR-TOF-MS	PTR-TOF-MS	PTR-MS
Methacrolein	GC-MS	GC-MS			PTR-MS
α-Pinene	GC-MS*		PTR-TOF-MS		GC-MS*
β-Pinene	GC-MS*		PTR-TOF-MS		GC-MS*
Limonene	GC-MS*				
Alkyl Nitrates					
Methyl Nitrate	GC-MS*	GC-MS			GC-MS*
Ethyl Nitrate	GC-MS*	GC-MS		GC-MS	GC-MS*
n-Propyl Nitrate	GC-MS*	GC-MS		GC-MS	GC-MS*
iso-Propyl Nitrate	GC-MS*	GC-MS		GC-MS	GC-MS*
n-Butyl Nitrate				GC-MS	
2-Butyl Nitrate	GC-MS*				GC-MS*

*indicated that VOCs were collected with canister first and then measured with GC-MS.

List of Acronyms in Table S7

CRDS – Cavity Ring Down Spectroscopy

GC-FID – Gas Chromatograph Flame Ionization Detector

GC-MS – Gas Chromatograph Mass Spectrometry

HR-TOF-MS – High Resolution Time-of-Flight Mass Spectrometry

PTR-MS – Proton Transfer Reaction Mass Spectrometry

PTR-TOF-MS – Proton Transfer Reaction Time-of-Flight Mass Spectrometry

References

Edwards, P.M., Brown, S.S., Roberts, J.M., Ahmadov, R., Banta, R.M., DeGouw, J. A., Dubé, W.P., Field, R. A., Flynn, J.H., Gilman, J.B., Graus, M., Helmig, D., Koss, A., Langford, A.O., Lefer, B.L., Lerner, B.M., Li, R., Li, S.-M., McKeen, S. A., Murphy, S.M., Parrish, D.D., Senff, C.J., Soltis, J., Stutz, J., Sweeney, C., Thompson, C.R., Trainer, M.K., Tsai, C., Veres, P.R., Washenfelder, R. a., Warneke, C., Wild, R.J., Young, C.J., Yuan, B., Zamora, R: High winter ozone pollution from carbonyl photolysis in an oil and gas basin. Nature, 514, 351-354, https://doi.org/10.1038/nature13767, 2014.

Hauglustaine, D.A., Granier, C., Brasseur, G.P., and Mégie, G.: The importance of atmospheric chemistry in the calculation of radiative forcing on the climate system. Journal of Geophysical Research, 99, doi:10.1029/93JD02987.issn:0148-0227, 1994.

Knote, C., Tuccella, P., Curci, G., Emmons, L., Orlando, J.J., Madronich, S., Baró, R., Jiménez-Guerrero, P., Luecken, D., Hogrefe, C., Forkel, R., Werhahn, J., Hirtl, M., Pérez, J.L., San José, R., Giordano, L., Brunner, D., Yahya, K., Zhang, Y.: Influence of the choice of gas-phase mechanism on predictions of key gaseous pollutants during the AQMEII phase-2 intercomparison. Atmospheric Environment, 115, 553-568, https://doi.org/10.1016/j.atmosenv.2014.11.066, 2015.

Levelt, P.F., Hilsenrath, E., Leppelmeier, G.W., Oord, G.H.J. van den, Bhartia, P.K., Tamminen, J., Haan, J.F., and de Veefkind, J.P.: Science objectives of the ozone monitoring instrument. IEEE Trans. Geosci. Remote Sens. 44, 1199-1208, https://doi.org/10.1109/TGRS.2006.872336, 2006.